UNIVERSITY OF FORESTRY
FACULTY OF FORESTRY
DEPARTMENT OF DENDROLOGY

Abstract of

DISSERTATION

for scientific level
"DOCTOR OF SCIENCE"

in a science area
6. "AGRICULTURAL SCIENCE AND VETERINARY",

professional field

6.5 "FORESTRY",

scientific specialty

"FORESTRY (INCL. DENDROLOGY)"

on the topic:

PHYSIOLOGICAL ACCLIMATION OF EUROPEAN BEECH

Author:
Assoc. Prof. Svetoslav Mladenov Anev, PhD

Sofia, 2024 г.

HEAD 1. INTRODUCTION

The adaptation of living organisms is a species-specific process. It is achieved through the mechanisms of natural selection – individuals best adapted to the environment survive to reproductive age – those that have the most significant match between their ecophysiological capabilities and the variations of the environment. Only they take part in reproduction, and the transmission of their genetic qualities to the generation, and thus, this match is strengthened at the species level (Lambers & Oliveira 2019; Schulze et al. 2019). This process is slow, especially for long-lived tree species that build forests, characterised by a long growth period and late entry into the reproduction stage. The change of generations in a forest takes decades, and not rarely more than a hundred years, and this makes adaptation slow.

On the other hand, acclimation is a characteristic of individuals, which is realised within the framework of their genetic potential and individual duration of existence (Lambers & Oliveira 2019). It represents an adjustment to stress provoked by fluctuating environmental factors (Schulze et al. 2019). The most rapid biochemical changes occur, such as a change in the balance of phytohormones, redirection of resources for synthesising protective compounds – enzymes, terpenes, phenols, flavonoids, etc.; accumulation of reserve substances, etc. These biochemical changes cause a cascade of changes occurring at the physiological level, such as a change in the balance between photosynthesis and respiration, compromises related to the water regime and mineral nutrition, and changes in growth and reproduction. At a later stage, the changes are reflected at the anatomical and morphological level (Schulze et al. 2019). Some species, such as the European beech, form typical sun and shade leaves – significantly different in their structure – which helps them absorb resources more efficiently under the relevant light conditions (Naidu & DeLucia 1998; Kraj & Ślepaczuk 2022). This change can be annual because the species has invested in the formation of winter buds since the summer (July) of the previous year. However, this is associated with increased expenditure and redistribution of available resources. Although acclimation is not fixed at the genetic level and cannot be transmitted to generations (Lambers & Oliveira 2019), long-lived tree species that build the forest are key to their adaptation in the medium term to climate dynamics. From this point of view, the potential for physiological acclimation is of interest, and its knowledge can enrich the techniques of adaptive silviculture.

HEAD 2. GOAL AND TASKS

The general goal of the described experiments was to study acclimation mechanisms in European beech for adjustment to variations in specific environmental factors – abiotic (light intensity, air temperature, precipitation amount, mechanical damage from wind and/or ice, etc.) and biotic (damage from beech leafhopper larvae), intensified by climate change and human activity. These mechanisms have been studied at different levels – from the activity of biochemical enzymatic antioxidants and the synthesis of secondary metabolites as stress markers, through the elements of gas exchange determining the carbon and water balance of plants, to the formation of anatomically and morphologically different leaves and changes in essential phenological manifestations.

In the first described experiment, the aim is to conduct detailed studies on the changes in the assimilation activity, water regime and the state of the antioxidant defence system of European beech individuals affected by the *Orchestes fagi* L. to reveal the physiological and biochemical mechanisms of reaction and resistance to this pest. The tasks are related to determining the responses of European beech to the attack at different levels:

1. Determining the extent of damage;
2. Determining changes in the levels of gas exchange;
3. Determining changes in the activity of enzymatic antioxidants;
4. Determining changes in the content of non-enzymatic antioxidants.

The second experiment investigates mechanisms for light acclimation of the natural undergrowth in European beech forests, restored through silvicultural activities of different types and intensities or natural disturbance. To achieve the set goal, the following tasks were completed:

1. Determination of changes in the parameters of the light dependence of photosynthesis of European beech saplings after opening the canopy;
2. Determination of changes in transpiration and water use efficiency of European beech saplings after opening the canopy;
3. Determination of changes in carbon and light use efficiency of European beech saplings after opening the canopy;
4. Determination of changes in the content of plastid pigments in the leaves of European beech saplings after opening the canopy;
5. Determination of changes in the antioxidant defence system in the leaves of European beech saplings after opening the canopy;

6. Determination of changes in the balance of nitrogen and carbon in the leaves of European beech saplings after opening the canopy.

In the third described experiment, the dynamics of the vegetative phenological manifestations of European beech for 2017–2023 were tracked using remote sensing methods. The aim was to study the influence of different hydrothermal features of individual years on the phenology of forests with a predominance of European beech in two mountains of Western Bulgaria – Belasitsa and Western Stara Planina. The following tasks were completed to achieve the set goal:

1. Determining the annual course of the plant phenological index (PPI) for the studied forests using satellite images;
2. Studying the relationship between temperatures and precipitation in individual years and PPI levels;
3. Determining the parameters of the annual course of PPI for the two sites – the start of the growing season (SOSD), maximum of the growing season (MOSD), end of the growing season (EOSD) and length of the growing season (LOSD);
4. Study the relationship between the determined parameters of the annual course of PPI with altitude and latitude in both sites.

The main goal of the fourth described experiment is to track the dynamics of forest recovery in the Petrohan State Forest Reserve affected by the ice storm in 2021 through remotely determined vegetation indices. The following tasks have been formulated:

1. Determination of the dynamics of the normalized difference vegetation index (NDVI), the plant phenological index (PPI) and the leaf area index (LAI) in the affected forests for the period 2017 - 2023;
2. Determination of risk factors for ice storm damage in beech forests;
3. Determination of the recovery rates of the studied vegetation indices in the territory affected by the ice storm;
4. Determination of changes in the gas exchange of saplings affected by the destruction of the canopy.

The specific methods are dictated by the nature of the individual experiments, which investigated the acclimation potential of the European beech to biotic and abiotic stressors.

HEAD 3. OBJECTS AND METHODS

3.1. Experiment „Orchestes fagi“

3.1.1. *Objects*

The experimental plots were located in stands at two altitudes - EP-Shirine, in stand 195a and EP-Petrohan, in stand 94a.

Table 3–1. Characteristics of the experimental plots

Experimental plot	1 – Shirine	2 – Petrohan
Stand	195 a	94 a
Area, ha	14.9	26.8
Altitude, m	680	1450
Aspect	ЮЗ	ЮИ
Slope, °	22	18

3.1.2. *Methods*

3.1.2.1. Morphological analysis of leaves.

The leaves were the subject of physiological and biochemical measurements and were also used for morphological analysis. 15 leaves from each of the two sample areas were analyzed thrice in 2016 to determine the degree of attack by *Orchestes fagi*. After being torn off, the leaves were weighed on an electronic scale (0.01 g) and scanned with a Canon Lide 110 scanner at a resolution of 600 dpi. The files of the scanned leaves were processed using the ImageJ v.1.51f (x64) software program, through which the type of damage, the total area of the leaves, the percentage of healthy and the percentage of damaged area were determined (Anev et al. 2016).

3.1.2.2. Gas-exchange measurements.

The measurements were carried out using a Portable Photosynthesis System Li-6400 (Li-COR, Bioscience, Lincoln, NE, USA). The levels of the main physiological processes of the leaves were measured in the two experimental plots six times – in June, July, and August of the vegetation periods of 2015 and 2016. Model trees were selected for the measurements, on which 15 leaves with varying degrees of attack by the leaf-mining larva of the *Orchestes fagi* were selected from lighted and shaded crown levels. During the measurements, the levels of the environmental factors were maintained constant and within optimal limits for the gas-exchange (Table 3–2).

Table 3–2. Environmental factors in Li-6400 chamber

Environmental factors	Стойност по време на измерванията
PPFD, μmol(γ)·m^{-2}·s^{-1}	1000
Air temperature, °C	18-24
Relative air humidity, %	40-60
Flow rate, mol . s^{-1}	500

Water use efficiency (WUE) was calculated as the ratio between the measured photosynthesis and transpiration rate. The obtained results were subjected to statistical analysis - Shapiro-Wilk test for normality of distribution, $p < 0.05$; descriptive statistics; One-way ANOVA with

subsequent Holm-Sidak test for the reliability of the differences between the levels of the studied physiological indicators at different degrees of attack.

3.1.2.3. Biochemical analysis.

The analyses were performed on the leaves fixed in liquid nitrogen in the field. The enzymatic antioxidants were determined as superoxide dismutase activity (Beauchamp & Fridovich 1971), catalase activity (Aebi 1984) and peroxidase activity (Hart et al. 1971). The total antioxidant activity was determined according to Prieto et al. (1999). The changes in the amount of phenols (Singleton et al. 1999) and flavonoids (Chang et al. 2020) in beech leaves observed due to the attack of the beech gall midge were determined.

3.1.2.4. Macro- and microelements in leaves.

The analyses were performed using the Kjeldahl method, colourimetric and atomic adsorption analysis after the combustion of the plant samples (Jones 1991).

3.2. Experiment „light acclimation“

3.2.1. *Objects*

The physiological responses of European beech (*Fagus sylvatica* L.) saplings to canopy opening were studied at the Petrohan forests in the Western Stara Planina. The experimental sites were located in European beech-dominated forests, ranging between 700 and 1450 m. The sites were selected according to their different silvicultural history or natural disturbances which affected them. Each site included two test plots with dimensions of 25 / 40 m – one in a stand with an open (O-plot) canopy from logging or natural disturbance and one in a closed (C-plot) canopy, playing the role of control for comparison of the response to canopy opening. In 2011, the stand in 93a was opened by cutting for transformation into a group-selective stand. All adult (120 years old) trees in the patch measuring about 0.1 ha were felled. The size of the patch was not changed subsequently. (NIS-LTU 2018). In a mature stand (143c) at 1000 m above sea level in 2013, gaps for group-gradual cutting were opened, in one of which, with a size of ~0.5 ha in 2018, EP 2_O was set. In the neighbouring stand 143b, the control EP 2_C was established. In the autumn of 2014, in stands 7b and 7c, due to strong winds, about an 80-year-old beech forest, fell on an area of about 6 ha, in which EP 3_O was established (Table 3–3).

Table 3–3. Characteristics of experimental plots.

Experimental plots	Latitude, ° ′ ″	Longitude, ° ′ ″	Altitude, m	T_{AIR} °C	HD %	PPFD, µmol(γ)·m^{-2}·s^{-1}	n	N
EP 1_O	43°7′30″	23°7′23″	1450	21.07 ± 0.05	46.8 ± 0.2	912.7 ± 197.3	25	200
EP 1_C	43°7′32″	23°7′25″	1439	20.68 ± 0.07	56.6 ± 0.5	47.7 ± 5.8	22	176
EP 2_O	43°8′23″	23°8′37″	1015	23.56 ± 0.10	56.5 ± 0.4	773.2 ± 244.2	25	200
EP 2_C	43°8′22″	23°8′33″	970	22.72 ± 0.03	55.8 ± 0.2	39.0 ± 12.2	22	176
EP 3_O	43°11′18″	23°7′33″	862	26.45 ± 0.14	46.3 ± 0.5	1125.5 ± 186.5	23	184
EP 3_C	43°11′15″	23°7′32″	870	24.25 ± 0.11	59.2 ± 0.5	163.1 ± 95.2	20	160

EP 4_O	43°9′27″	23°8′59″	718	26.22 ± 0.06	58.6 ± 0.4	385.2 ± 42.2	25	200
EP 4_C	43°9′29″	23°9′00″	713	25.11 ± 0.07	57.6 ± 0.3	171.5 ± 10.7	25	200

The control area EP 4C has been established in permanent experimental area 12 of the Forest Management Department (stand 155d). In the neighbouring stand 155e, where Shelterwood harvest has been carried out, EP 4_O has been established.

3.2.2. *Methods*

3.2.2.1. Light-curve of photosynthesis

Each experimental plot was divided into 100 plots measuring 2.5×4.0 m. Three plots were randomly selected from these plots, in which the intensity of photosynthesis, respiration and transpiration were measured three times during the growing season. The measurements were carried out with an automatic infrared gas analysis system Li-6400 (LiCor Bioscience, Lincoln, NE, USA) using a standardized methodology for constructing the light dependence of photosynthesis, according to the protocol of Evans & Santiago (2014). The data from each experimental plot were processed with a specially created VB script for nonlinear regression using the Levenberg-Marquardt algorithm to minimize errors. With the obtained values for maximum photosynthetic rate (A_{MAX}), respiration rate (R_D) and transpiration rate (E), the water use efficiency WUE = A_{MAX}/E and the carbon use efficiency CUE = A_{MAX}/R_D were calculated. Light use efficiency (LUE), light compensation point (LCP) and saturating light were obtained directly from nonlinear regressions of the light curves. The light curve of each leaf was analyzed separately. The results of the biological replicates were further analyzed with descriptive statistics tools. The studied indicators were tested for the significance of differences using One-Way ANOVA, followed by Holm-Sidak post-hoc analysis at p-value < 0.05.

3.2.2.2. Photo fluorescence

One of the most precise devices for measuring photofluorescence parameters is the Li-600, manufactured by LI-COR Bioscience (Lincoln, NE, USA). The LI-600 is a compact fluorometer with pulse amplitude modulation (PAM). For plants in natural conditions, including light, the Li-600 measures the quantum yield of photosystem two or the fraction of light used to drive biochemical processes in the dark phase of photosynthesis Φ_{PSII} = (Fm' – FS)/ Fm', where: Φ_{PSII} is the quantum yield of photosystem 2, Fm' is the maximum fluorescence yield, and Fs is the steady-state fluorescence.

3.2.2.3. Biochemical markers

The content of chlorophyll "a", chlorophyll "b" and carotenoids was determined by the method of Arnon (1949) after extraction with 80% acetone. The total phenolic content was determined by the method of Singleton et al. (1999), and the total flavonoid content by the method of Chang et al. (2020). The superoxide dismutase (SOD) activity was determined by the method of

Beauchamp & Fridovich (1971). The enzyme catalase (CAT) activity was determined by Aebi's method (1984). The guaiacol peroxidase (GPX) activity was determined by the method of Hart et al. (1971). The total antioxidant activity was determined by the method of Prieto et al. (1999).

3.3. Experiment „phenology"

3.3.1. *Objects*

The dynamics of the vegetative phenological manifestations of European beech were monitored for 2017–2023 using remote sensing methods. Twelve thousand four hundred thirty-two stands with European beech domination from 2 areas were analyzed: Petrohan State Forest Reserve (n = 7,525) and Petrich State Forest Reserve (n = 4,907). The two mountains in which the stands were selected for the analysis have different latitudes, a much smaller difference in longitude, a wide altitudinal gradient, and a diversity of forests by age (Figure 3–1).

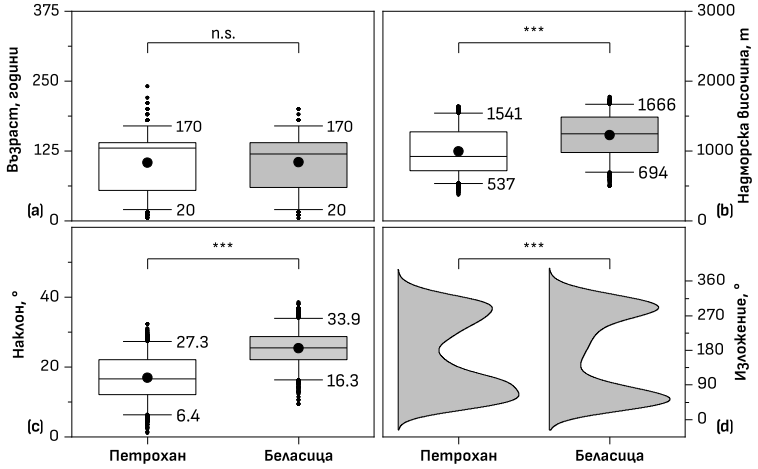

Figure 3–1. Age and orography of the objects. (T-test, *** P-value < 0.001; n.s. P-value > 0.05).

The average age of the forests with a predominance of European beech is 104.2±0.6 years for Petrohan and 104.4±0.7 years for Belasitsa, respectively. 90% of the forests in both sites are between 20 and 170 years of age, with the main difference being in the several stands in the old age phase of Petrohan, one of which reaches 250 years. The average altitude of the forests with a predominance of European beech for Petrohan is 989.6 ± 3.7 m, and for Belasitsa, it is significantly higher (p-value < 0.001) – 1222.4 ± 4.4 m. 90% of the European beech forests in Petrohan are between 537 and 1541 m asl, and in Belasitsa – between 694 and 1666 m asl. The northern slopes of the Western Balkan Mountains in the Petrohan region are significantly steeper (p-value < 0.001) compared to those of Belasitsa.

3.3.2. *Methods*

3.3.2.1. Phenology

Multispectral satellite images captured by the Sentinel-2 satellites of the European Space Agency (ESA) Copernicus program were used to track phenological rhythms, the effects of natural disturbances and logging in forests in the studied areas.

1) The daily values of four vegetation indices – NDVI, LAI, FPAR, and PPI- are calculated automatically from images captured by the Sentinel-2 satellites.
2) Seasonal trajectories of the plant phenological index (PPI) are a 10-day time series of PPI obtained from a regression model for smoothing the index's raw data. The regression model is a double logistic function proposed by Fischer (1994) and adapted by Beck et al. (2006) for multi-year dynamics of vegetation indices, which was improved by Jönsson et al. (2018).

$$PPI_{DOY} = PPI_{MIN} + \sum_{i=1}^{n}\left[\left(PPI_{MAX} - PPI_{MIN}\right)\cdot\left(\frac{1}{1+e^{\frac{SOSD-DOY}{L_{Slope}}}} - \frac{1}{1+e^{\frac{EOSD-DOY}{R_{Slope}}}}\right)\right]$$

Where: SOSD and EOSD are the date of mass leafing and the date of mass leaffall for deciduous species, respectively, and of a permanent increase and a permanent decrease in photosynthesis for evergreen species. L_{Slope} and R_{Slope} are the regression slopes in spring and autumn; DOY is the day of the year, and PPI_{MAX} and PPI_{MIN} are the maximum and minimum PPI values for the respective year, respectively.
3) Plant Phenology and Productivity (VPP) includes 13 yearly parameters.

3.3.2.2. Images preparation and processing

Sentinel-2 satellite images with 10 m spatial resolution were downloaded from the Wekeo website (https://www.wekeo.eu/) and from the vito.be server. Post-processing was performed in open-source GIS software (QGIS v.3.32.3). A Python script was used to determine the raster data values falling within the vector polygons of individual farms, departments and sub-departments. Subsequently, the tools of the built-in raster analysis packages were used, as well as the tools in GDAL (v.3.7.2) and GRASS GIS (v.8.3.0). The resulting attribute tables were processed in MS Excel 2019 with the built-in functions, as well as with specially created VBA functions and scripts in MS Visual Basic for Applications (v.7.1).

3.4. Experiment „natural disturbances“

3.4.1. *Objects*

The study’s object was the stands in the Petrohan Forest damaged by the ice break of January 2021. A method has been developed for remote validation and assessment of similar damage in forest areas and the restoration rate of stands after damage.

3.4.2. *Methods*

The dynamics of several vegetation indices calculated from images captured in different years but on dates close to each other were tracked. Images captured in late July or early August, when plants are still in active vegetation, when active leaf senescence has not started, and, most

importantly, when the days are primarily cloudless, were preferred. The indices calculated with the built-in raster calculator were processed with the Zonal statistics tool in QGIS, using a Python script to automate the process. The mean value of the index, its standard error and the number of pixels involved in calculating the mean value were calculated at the stand's level. The values were exported to a CSV file for subsequent processing in MS Excel. The extent of damage was analysed on a background of altitude and exposure, forest type, main tree species, age and stand completeness, soil type and depth, as well as other indicators such as condition, slope, property and mechanical resistance, calculated as the ratio of the height of the main stand to the diameter at breast height (H/DBH). The acclimation of European beech saplings to drastically changed environmental conditions was assessed by measuring gas exchange elements and constructing photosynthesis's light dependence.

HEAD 4. RESULTS AND ANALYSIS

4.1. Reaction to the *Orchestes fagi* infestation

The damage observed in the two sample plots was of different magnitudes. The average percentage of damaged leaves in the lower-lying EP Shirine was 21.56%, which was 3.18 times higher than the damage observed in EP Petrohan—6.79% (Figure 4–1).

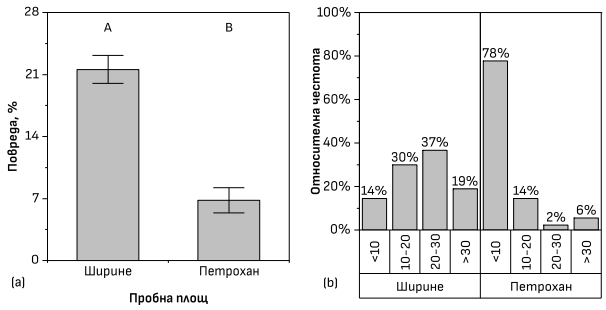

Figure 4–1. Amount of damage (%) caused by *Orchestes fagi* (a) and its distribution by degree (b).

In EP-Petrohan, more than ¾ of the leaves are practically unaffected by the *Orchestes fagi*, and only under 8% of the leaves have damage exceeding 20%. In contrast, in EP-Shirine, more than half (56%) of the leaves have damage exceeding 20%, and only 14% were slightly affected. For comparison, in the period 2004–2006, Dimitrova-Mateva (2008) reported for the Petrohan an average size of the damaged leaf area of the order of 7.5–9.0% with between 60 and 80% of the beech leaves. At higher altitudes, beech forms leaves with denser mesophyll, thicker cell walls and thicker cuticles as a protective reaction to harsher conditions (Adamidis et al. 2021). According to Peeters (2002), this probably further complicates larvae' feeding. At lower altitudes (EP-Shirine), conditions stimulate the rapid development of the Orchestes fagi and cause significant changes in the leaves' metabolic composition and physiological activity (Figure 4–2).

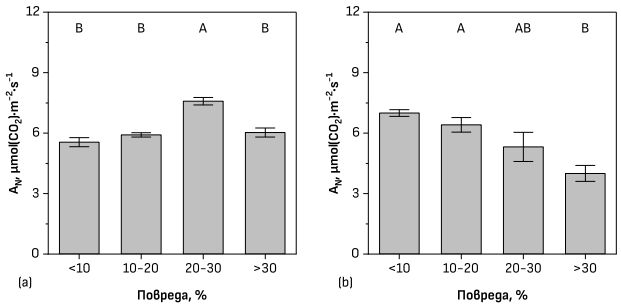

Figure 4–2. Photosynthetic rate (A_N) of leaves with different damage (a) EP-Shirine and (b) EP-Petrohan.

In the EP-Shirine, the level of photosynthesis increases with increasing leaf attack to 20-30%, after which it decreases. This effect of compensating for damage by the leaf's healthy part has been established by us (Anev et al. 2015) and by other authors (Retuerto et al. 2004). Such an effect is not observed in the EP-Petrohan (1450 m above sea level). With increasing infestation rates, photosynthesis there permanently decreases, and at infestation rates above 30%, it is already significantly lower than that of less damaged leaves. The lack of potential for compensating for damage in the healthy part of the leaves in this sample area is probably due to the accompanying stress from the more extreme fluctuations in environmental factors (temperature, solar radiation, precipitation) at this higher altitude. Still, it can also be found in the rarer and more occasional encounters with the pest. The intensity of transpiration (E) in PP-Shirine is highest in the least affected leaves and significantly lower but constant in the following three degrees of infestation, in contrast to the "uncontrollable" transpiration reported by other authors (Lazarev et al. 2001) in leaves damaged by *O. fagi*.

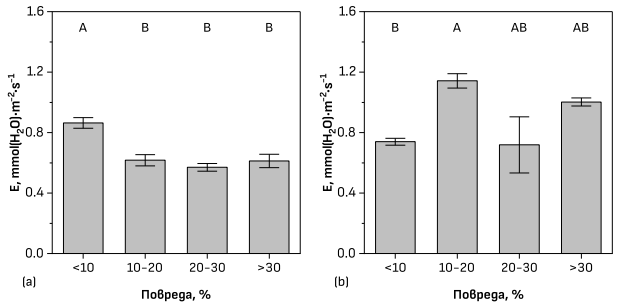

Figure 4–3. Transpiration rate (E) of leaves with different damage (a) EP-Shirine and (b) EP-Petrohan.

The loss of leaf surface and the tendency to conserve water in this hotter test area are the likely reasons for the reduction in E with increasing attack. Still, the leaves fail to maintain this tendency even at greater than 20% damage. The transpiration of saplings in EP-Petrohan is more dynamic, and damage levels above 10% of the leaf area are significantly higher than those in EP-Shirine. The higher humidity in this EP explains the high intensity of transpiration, and its increase with increasing damage is probably due to the evaporated water from the damaged areas – an effect that can only be observed when water is abundant (Figure 4–4).

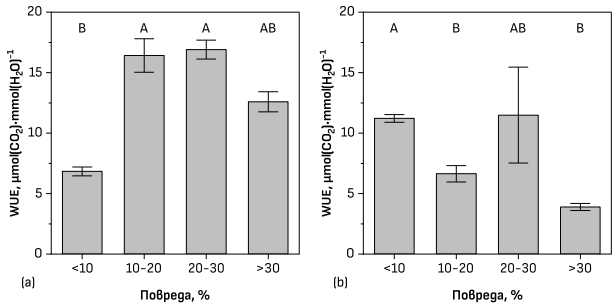

Figure 4–4. Water-use efficiency (WUE) of leaves with different damage (a) EP-Shirine and (b) EP-Petrohan.

The water-use efficiency, as a function of the two elements of gas exchange (A_N and E), in EP-Shirine at a low infestation (up to 10%) is low, increases with increasing infestation degree (up to 30%), and in the most damaged leaves (over 30%) it decreases again but still maintains higher levels than those in the least affected ones. The explanation of this specific trend is, again, the probable compensatory effect that the healthy part of the leaves has at optimal levels of microclimatic factors. In EP-Petrohan, despite the significant variation of WUE in the third infestation degree, the trend of decreasing WUE with increasing infestation degree is visible.

The results obtained from the biochemical analyses show the presence of changes in the antioxidant defence system of the European beech. Superoxide dismutase (SOD) has a significantly higher activity in the leaves of beech trees in EP-Shirine, compared to EP-Petrohan. On the other hand, catalase activity is higher in EP-Petrohan, which leads to assuming different strategies for enzymatic antioxidant protection at various altitudes. If in the warmer and drier EP-Shirine, SOD is the primary enzymatic antioxidant. In EP-Petrohan, catalase has to work more actively to clean up free oxygen radicals accumulated at the end of the light phase of photosynthesis and at the beginning of its dark phase (Figure 4–5).

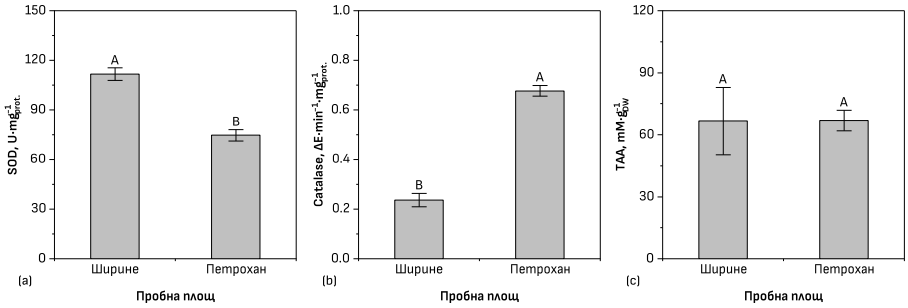

Figure 4–5. Changes in (a) superoxide dismutase activity, (b) catalase activity, and (c) total antioxidant activity in European beech (*Fagus sylvatica* L.) leaves.

H_2O_2 is formed during the photorespiration process, which is significantly more intense under intense light and low atmospheric pressure – abiotic stress factors that are more associated with EP-Petrohan than with EP-Shirine, and this explains the higher activity of catalase. Thus, the total antioxidant activity of the enzymatic antioxidants (TAA) is equalized in the two test areas, with a different strategy for maintaining its levels. Dimitrova-Mateva (2008) found similar

increased activity in damaged leaves of catalase and SOD in May, which, however, is depleted by August. In contrast, in peroxidase and glutathione reductase in the attacked leaves, the activity is higher in August, which confirms the assumption of a specific strategy for activating the enzymatic defence.

In EP-Petrohan, in the two months of active feeding of the insect (June and July), phenols increased 1.35 times, and in EP-Shirine, they increased more than 4.54 times. In the case of flavonoids, the differences are small – in July, compared to June, 1.73 times more flavonoids were recorded in EP-Shirine and 2.87 times in EP-Petrohan (Figure 4–6).

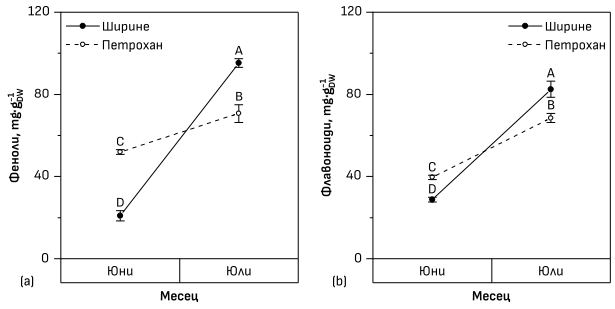

Figure 4–6. Total phenols (a) and flavonoid contents (b) in leaves.

The results show that the pathogen feeding does not adversely affect phenolic biosynthesis. Still, no increased phenolic content was found in the more affected leaves in June, in contrast to the results of Dimitrova-Mateva (2008), who found a higher content of phenols after the attack of the *Orchestes fagi* and throughout the growing season. The amount of total phenolic compounds increases during the growing season, and although it is higher in the leaves in PP-Petrohan in June, it reaches a maximum in PP-Shirine in July. The flavonoid content increases and reaches a maximum in July in the leaves from the lower EP-Shirine (83 mg g^{-1}_{DW}). From the results obtained, it can be concluded that at optimal levels of microclimatic conditions, the European beech can compensate for the attack of the *Orchestes fagi* by increasing the physiological activity of the healthy part of the leaf petioles. At more extreme environmental factors, this ability to compensate for damage weakens or is not observed and physiological processes become destabilized.

4.2. Light acclimation

4.2.1. *Photosynthetic changes with light changes*

In all open-canopy (O) plots, the photosynthetic light curves are typical of a sunny leaf ecotype, and in most of the closed-canopy (C) control plots, they are typical of a shaded leaf ecotype. Photosynthesis is light-saturated, reaching 90% of its maximum at PPFDs between 250 and 500 $\mu mol(\gamma) \cdot m^{-2} \cdot s^{-1}$ for shaded leaves of plants in C-plots. At the same time, sunny leaves in O-plots require significantly lighter and their photosynthesis is saturated at PPFDs > 1000 $\mu mol(\gamma) \cdot m^{-2} \cdot s^{-1}$. The difference is most significant at 1000 m above sea level and decreases

with increasing or decreasing altitude. The light curves of O and C intersect (i.e., net photosynthesis $A_N = A_G - R_D$ in both areas equalizes) in PP 1 at 36 µmol(γ)·m^{-2}·s^{-1}, in PP 2 at 59 µmol(γ)·m^{-2}·s^{-1}, in PP 3 at 51 µmol(γ)·m^{-2}·s^{-1}, and in PP 4 this occurs at 84 µmol(γ)·m^{-2}·s^{-1}. The smooth increase of this indicator with decreasing altitude is disrupted only in the windward PP 3, probably due to plant stress (Figure 4–7).

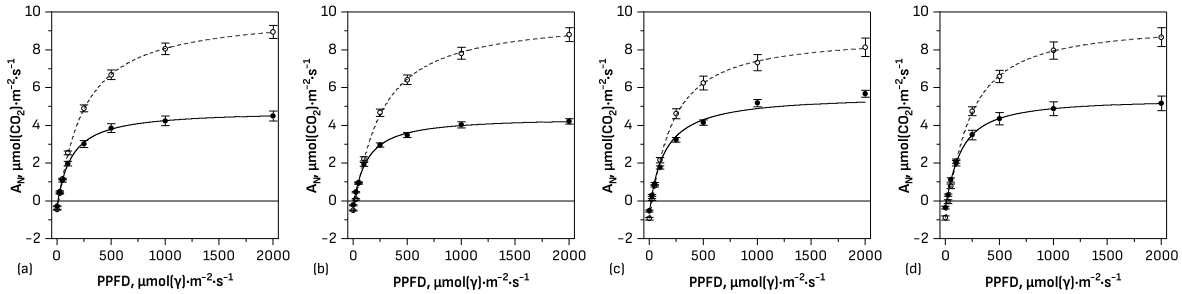

Figure 4–7. Photosynthetic light curves of plants in the O-plots (- ○ -) and in the C-plots (–●–) in a) PP 1, b) PP 2, c) PP 3 and d) PP 4. The mean values (n > 20) of net photosynthesis (A_N) at different light levels (PPFD) are shown by dots, and whiskers indicate their standard errors (±SE). Lines show the regression relationships.

Only exceptionally, in single leaves from the C-plots was a photoinhibitory effect observed, i.e. a lower intensity of photosynthesis at 2000 µmol(γ)·m^{-2}·s^{-1}, compared to that at 1000 µmol(γ)·m^{-2}·s^{-1}. In PP 3, not only are the plants in the wind-exposed area under stress and cannot realize a light curve, as observed in the other PPs, but also in the control PP 3C, probably due to the drier air, soil drainage and increased air temperature, as a result of the increased albedo of the adjacent forest-exposed wind-exposed area, the light curve is not typical of a shady leaf ecotype, but is relatively transient. In PP 4, a similar convergence of the light curves is observed, which is, however, due to the weaker opening of the canopy due to the short-term gradual felling and the much more similar conditions between the C and O areas. In PP 2 and especially in PP 1, where the scales of the open windows are more extensive and, as a result, significantly more light is transmitted to the undergrowth, the distance between the light curves in the O and C areas is significant which is consistent with the findings of Wyka et al. (2007) for a good light acclimation potential of European beech in the event of incidental opening of the canopy. The latter is also evident from the comparison of the regression parameters of the light curves.

4.2.2. *Maximum photosynthetic capacity and dark respiration*

For example, the maximum photosynthetic capacity (A_{MAX}) in PP 1_O is 2.05 times higher than in PP 1C. For PP 2, this ratio is even 2.21 times, and in PP 4, it decreases to 1.77 times. In the windward area PP 3, the difference between the A_{MAX} of the two plots is only 1.45 times. On the other hand, A_{MAX} is relatively stable in the O-areas in the three types of felling and is slightly lower in the windthrow area, which is again a marker for stress in the saplings there. In the

folded controls (C-areas), A_{MAX} is low at lower temperatures at 1400 and 1000 m above sea level and increases slightly (up to 20%) in PP 4, which is at the lowest sea level. More serious (up to 43%) is the increase in PP 3_C, where warmer air from the windward territory probably penetrated the neighbouring compacted stands (Figure 4–8).

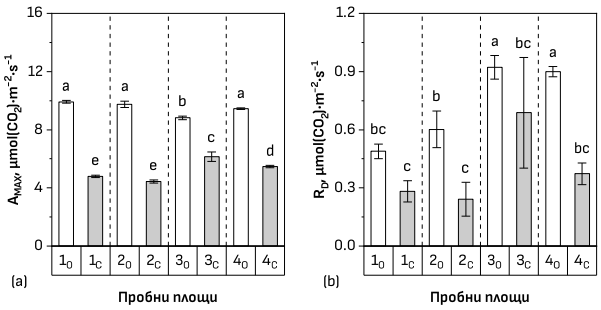

Figure 4–8. Maximum photosynthetic capacity (a) and dark respiration (b).

Čater & Levanič (2013) found a logarithmic relationship between the illumination in the sapling habitat and A_{MAX} significantly more pronounced than the silver fir, which is probably the reason for the observation of more intensive respiration, although without a significant difference, in PP 3, compared to PP 4. The linear relationship between R_D and the temperatures recorded during the measurements, shown in Table 3–3, is high (R^2 = 0.53, P-value = 0.035) and, although in the compact stands the differences are insignificant (probably due to more similar temperature conditions and/or due to species specificity in this indicator in the shady leaves), in the O-plots at 700 m (by up to 54%) and especially in the windward area (by up to 90%).

4.2.3. *Light compensation point and light saturation point*

Temperature and strongly related respiration are likely the factors that determine the dynamics of the light compensation point (LCP). The differences in LCP in individual PPs follow the same logic as in R_D (Figure 4–9).

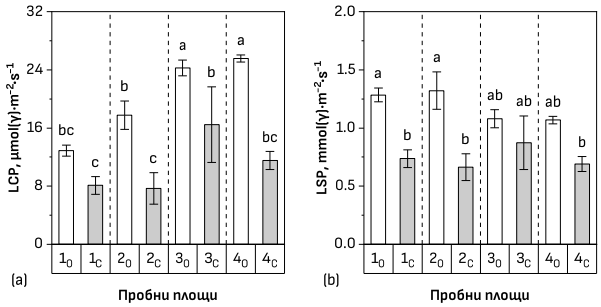

Figure 4–9. Light compensation point (a) and light saturation point (b).

It is worth noting that if 8–12 µmol(γ)·m^{-2}·s^{-1} is sufficient for the undergrowth under the canopy to equalize A_{MAX} and R_D, then in the open spaces after logging, LCP increases by 1.6 to 2.3 times and reaches over 25 µmol(γ)·m^{-2}·s^{-1}. The situation is similar to the saturation light (LSP), at which photosynthesis reaches 85% of Amax. Under the canopy, saturation is reached within a relatively narrow range of illumination – about 740.9±9.3 µmol(γ)·m^{-2}·s^{-1}, which indicates that this parameter is not so strongly influenced by altitude and the associated air temperature.

A linear relationship between natural illumination and the light compensation point, regardless of the type of logging, was established by Čater & Levanič (2013). In the O-plots, where the canopy was opened into windows by felling (PP 1_O and PP 2_O), the saturating light was significantly higher compared to that in the controls – 1283.5 and 1320.3 μmol(γ)·m^{-2}·s^{-1} for PP 1_O and PP 2_O, respectively. With the uniform thinning of the canopy in PP 4_O with short-term gradual felling, this difference decreases and becomes insignificant. Of interest is the weaker acclimation to intense light in the windward PP 3_O, where LSP also does not differ and is even closer to that in the control, which can be considered a signal of stress in the illuminated saplings. Still, it may also be due to lateral penetration of more light into the control, which may have led to some light acclimation of the saplings.

4.2.4. *Light- and carbon-use efficiency*

At the same time, carbon use efficiency (CUE), calculated as the ratio of A_{MAX} to R_D, did not differ significantly between O and C in any test plots. Although CUE in stands with open canopy decreases with decreasing altitude, probably due to the higher destructive element of the carbon balance – R_D, the values of this indicator in O-plots remain within the range of CUE variation in the corresponding C-plots. The latter can be considered on the one hand as a species-specific characteristic, but on the other hand – as a sufficiently broad acclimation potential of the sapling to adapt to canopy disturbances from a very early age, even when they are of more significant dimensions, as is the case in PP 3 (Figure 4–10).

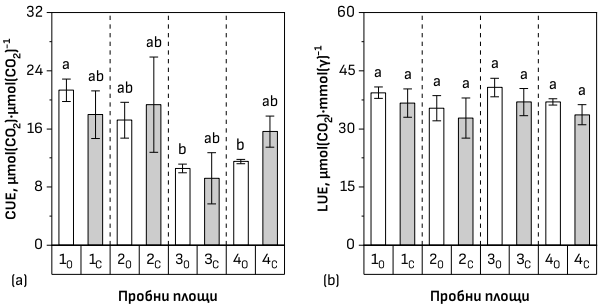

Figure 4–10. Carbon- (a) and light- (b) use efficiency.

Similar to the carbon use efficiency and the light use efficiency of another environmental resource – light (LUE) – does not show significant dynamics in individual PAs. Although there are slight differences between individual PAs, especially in O-plots, LUE emerges as a species-specific indicator and does not change significantly with a change in the light regime. Similar results are obtained for beech saplings after a sharp illumination from a natural disturbance. Unlike fir saplings, where LUE decreases exponentially with increasing illumination, it is maintained and even slightly increased in saplings of European beech and spruce (Čater 2021). On the one hand, European beech tends to form typical sunny and shady ecotype leaves with different characteristics. Still, on the other hand – these differences in the structure often act

oppositely at the physiological level and neutralize or at least disfigure the effect of others (Terashima et al. 2006). For example, the shade ecotype leaves have more chloroplasts in a single mesophyll cell, but due to the thinner leaf blade, the efficiency of photon absorption is similar. According to Genty et al. (1989), the efficiency of action or quantum yield of photosystem 2 (Φ_{PSII}) is one of the most reliable markers of light acclimation. The leaves of plants in the C-plots have an average value of $\Phi_{PSII} = 0.713 \pm 0.008$, and only in PP 4_C is it below 0.7 – 0.698 ± 0.007. With a similar quantum efficiency, $\Phi_{PSII} = 0.672 \pm 0.019$ are the leaves of individuals in PP 4_O, while in the other O-plots, Φ_{PSII} is significantly lower (Figure 4–11).

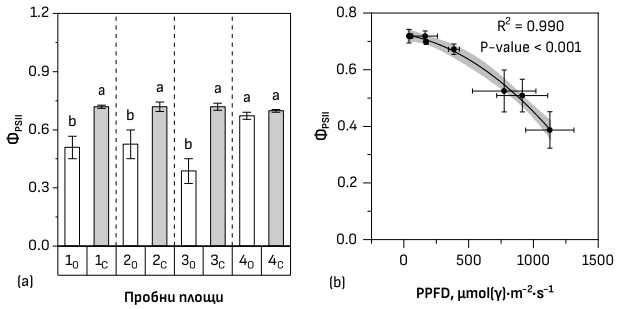

Figure 4–11. Quantum yield of photosystem II (Φ_{PSII}) (a) and relation between PPFD and Φ_{PSII} (b).

In the window opened during the valley-gradual felling (PP 2_O) $\Phi_{PSII} = 0.525 \pm 0.074$, in the window of PP 1_O $\Phi_{PSII} = 0.509 \pm 0.058$, and the windward PP 3_O $\Phi_{PSII} = 0.387 \pm 0.064$. The decrease in the quantum yield of photosystem two under more drastic disturbances of the structure shows that light acclimation cannot occur so quickly at the photochemical level. The relationship between Φ_{PSII} and incident light in PP is parabolic and very strong. Zha et al. (2017) point out that temperature is the factor that determines the slope of the regression relationship between light intensity and Φ_{PSII}. According to them, the slope of the regression is slightest under conditions of extreme drought (VPD > 1.5 kPa) and high temperature (> 24 °C). Similar results were reported by Ralph et al. (2007) for aquaculture. Havaux & Gruszecki (1993), and later by Ač et al. (2015), indicated that lower temperature probably leads to lower thylakoid membrane permeability, which may be the reason for the increased sensitivity of Φ_{PSII} to variations in light. Furthermore, reduced stomatal conductance under intense light, associated with the drive to conserve water, leads to a decrease in concentration of CO_2 in the intercellular space. Thus, water stress may negatively affect Φ_{PSII} (Jia et al. 2014).

4.2.5. *Water regime*

The water regime of beech saplings is significantly less affected by the canopy's opening compared to their carbon balance. The gradual increase in transpiration (E) with decreasing altitude, evident in the C-plots, is probably related to increasing temperatures with decreasing altitude.

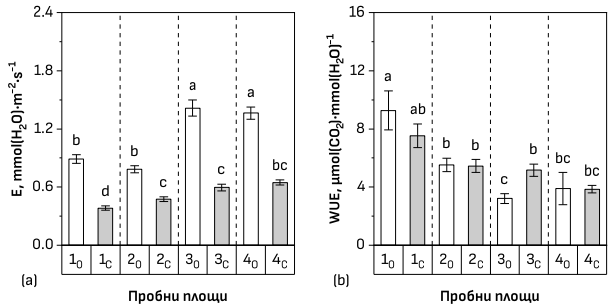

Figure 4–12. Transpiration rate (a) and water-use efficiency (WUE) (b).

This trend, however, is not realized in the O-areas. There, E is everywhere more intense compared to the C-areas, but in the more moderately arranged PP 2_O, this difference is 1.65 times; in the cooler, but with a more radical opening of the canopy PP 1_O, the difference is 2.32 times. The situation is similar in the other two PPs. In PP 4_O, which is at the lowest altitude, but only ~30% of the adult trees have been cut down, the difference is 2.11 times, and in the windy PP 3_O, this difference is already 2.38 times. Due to the different types and sizes of silvicultural interventions or natural disturbances, the changed transpiration has an impact, albeit weaker, compared to that in photosynthesis, on the water use efficiency (WUE). The general trend reflected by the control sample plots is that WUE decreases with decreasing altitude due to the increase in temperature and – as a result – increased evaporation in the lower parts of the mountain. In addition, the lack of significant differences between the O and C plots is striking. The most considerable anomaly in this trend is visible in PP 3_O, where WUE is significantly lower (1.61 times) than in PP 3_C. Based on the primary processes on which WUE depends, namely A_{MAX} and R_D, it can be said that although A_{MAX} in PP 3_O is lower compared to the other O plots, it is precisely here that the most intensive respiration, provoked by high temperatures is observed, due to the large size of the natural disturbance. , although Petkova-Tsokova (2019) found that the survival rate in geographic cultures of European beech is more related to the conditions of the growing site than to the specific origin, with the most significant being the importance of the rainfall regime, the influence of the opening of the canopy does not negatively affect primary water exchange processes.

4.2.6. *Chlorophyll content*

When analyzing the changes in the number of plastid pigments, a dynamic was observed, for which the limiting factor was not the altitude but another factor. Lichtenthaler et al. (1981) indicated that leaves adapted to high light have more chlorophyll per unit leaf area compared to the shaded ecotype of leaves, probably due to thicker leaf blades and more chlorophyll-bearing cells in the thicker mesophyll, especially in its palisade zone, which is two-rowed in sunny leaves and only one row in shaded leaves. At the same time, shaded leaves contain more chlorophyll than sunny ones per unit leaf mass, which was the method used in the present

experiment. In PP1, PP2 and PP3, the total chlorophyll content (chlorophyll “a” + chlorophyll “b”) is significantly higher in C-plots compared to O-plots. However, in PP 2, the differences are not as significant (4%) as in PP1 (22%) and even more so in PP3 (44%).

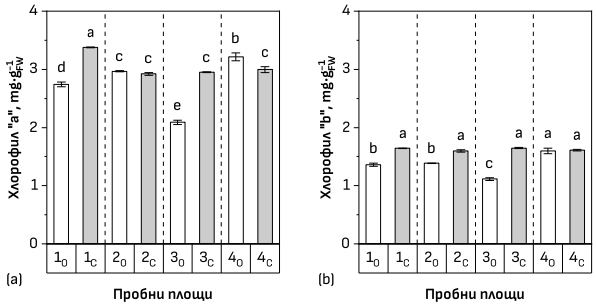

Figure 4–13. Chlorophyll “a” (a) and chlorophyll “b” (b) content.

Such tendency is probably due to both the higher content of chlorophyll “a” (23% and 41% times difference in PP1 and PP3, respectively) and the higher content of chlorophyll “b” (21%, 15%- and 48%-times difference in PP1, PP2 and PP3, respectively). Chlorophyll “b” is more prevalent in plants in C-plots than in O-plots everywhere, although in PP4, this difference is insignificant. It is chlorophyll “b,” the pigment that absorbs blue light more efficiently, and its high concentration is a marker of acclimation to shading. From this point of view, its lowest levels, recorded in the windward PP 3_O, are a sign of the reverse process of acclimation of saplings to extremely high levels of illumination. For this reason, and because chlorophyll a and chlorophyll b concentrations in PP 3_O are low, the total chlorophyll concentration here is very low, which can be interpreted as a likely signal of stress. The other O-area in which the difference in total chlorophyll content is relatively high is PP 1_O, in which the open window is large enough (~0.1 ha) to cause similar stress (Figure 4–14).

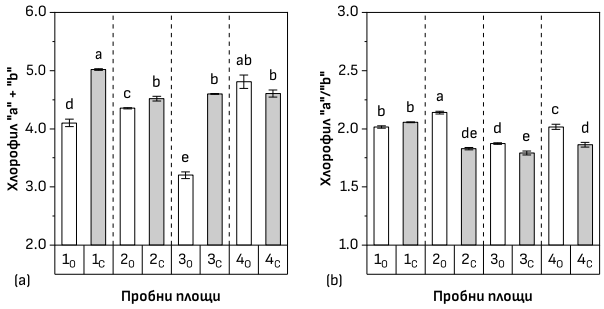

Figure 4–14. Chlorophyll “a” + chlorophyll “b” (a) and chlorophyll “a” / chlorophyll “b” (b).

The ratio between the two chlorophylls in the O-plots is significantly higher than in the C-plots only in the shelterwood harvests—PP 2_O and PP 4_O—which is a marker for the successful acclimation of the saplings to the changed illumination. In the other two PPs, the ratio is either similar, as is the case with PP1, or very close to that in the C-plot, as is the case with the wind-blown PP3.

4.2.7. *Antioxidant defence system*

In addition to the chlorophyll content and the balance of the two chlorophylls, the degree of acclimation can also be assessed by some stress markers, such as antioxidants, regardless of whether they are enzymatic or non-enzymatic.

4.2.7.1. Non-enzymatic antioxidants

The content of reducing sugars is higher in all O-plots than in their corresponding C-plots. There is a relatively well-pronounced tendency for more reducing sugars to accumulate at higher altitudes, which is also influenced by the degree of canopy opening. For example, the wind-blown PP 3_O equals this indicator in the less logging-affected PP 2_O, although it is at a full 150 m lower altitude. At the same time, the levels of reducing sugars are higher in PP 4_C, which can be explained by the slower uptake of photosynthetic products due to the relatively high efficiency of carbon uptake. Regarding carotenoid biosynthesis, differences between C and O areas are observed only in PP 1 and PP 2, which is probably related to the protective function of carotenoids in neutralizing photooxidative radicals, the mechanism of which is essentially the physical withdrawal of energy from the oxygen radical and its release through polyene vibration. In this way, carotenoids protect chlorophyll from photooxidation and photosynthesis from photoinhibition (Maoka 2020). The high content of carotenoids in PP 3C and PP 4C, comparable to that in the corresponding O-areas, may also be due to their action as signalling compounds for the synthesis of the stress hormone – abscisic acid (ABA) (Figure 4–10).

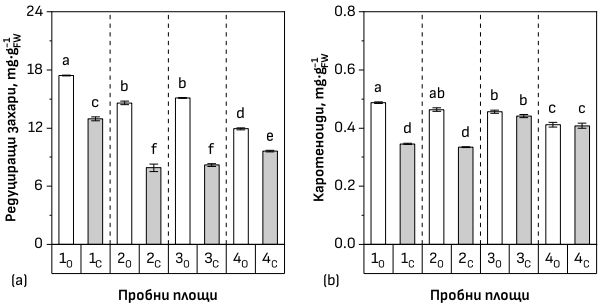

Figure 4–15. Reducing sugars (a) and carotenoids (b) content.

Activation of the biosynthesis of phenols and their derivatives – flavonoids – is observed due to the canopy's opening during felling or natural disturbance. One of the most significant benefits of anthocyanins (flavonoids) is protection from UV rays. Unlike other pigments (chlorophylls and carotenoids), anthocyanins are water-soluble and accumulate mainly in the vacuole. In spring, this happens in the vacuoles of the upper epidermis and palisade parenchyma, and later in summer – they migrate to the lower horizons of the leaf blade. In autumn, the biosynthesis of anthocyanins increases, and their role then is to preserve the

chlorophylls photoactive for a more extended period and thus ensure hardening for the winter. Phenols are in higher concentration in the leaves in the O-areas than in the C-areas, and the differences are related to the scale of the canopy opening. Their concentration in the wind-blown PP 3O is 2.31 times higher than in PP 3_C. For comparison, in PP 4_O, where short-term gradual logging was carried out, this difference with the corresponding PP 4_C is only 1.2 times. The trend is similar in the content of flavonoids, but while in PP 2 and PP 3 there are significant differences between the O and C areas, in PP 1 and PP 4 such differences are not observed. If, for PP 4_O, this reduced content of flavonoids is explained by the weaker opening of the canopy, then in PP 1_O, another factor probably intervenes since this is the area that is located at the highest altitude and, respectively, there is the higher amount of UV light and the need for protection as well (Figure 4–16).

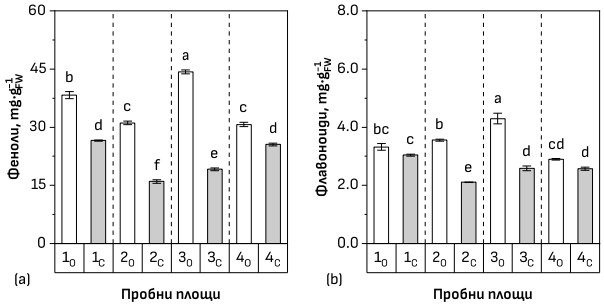

Figure 4–16. Phenols (a) and flavonoids (b) contents.

Given the significant amount of phenols present, it is evident that some factors are hindering the synthesis of flavonoids.

4.2.7.2. Enzymatic antioxidants

Enzymatic or "fast" antioxidants also increase their activity when the leaf is opened and exposed to increased light. Catalase, for example, is 5.18 times more active in leaves in the windward PP 3_O than leaves in PP 3C. In PP 1, this difference is 3.26 times, in PP 2 – 2.52 times, and the slightest difference is in PP 4 – 2.39 times (Figure 4–17).

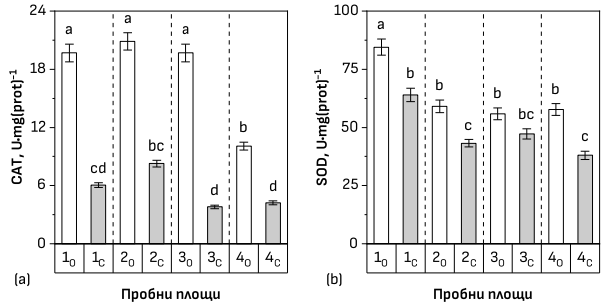

Figure 4–17. Catalase (a) and superoxide dismutase (b) activity.

This gradation fully corresponds to the size of the intervention in the plot and the change in the light regime compared to the control plots. As mentioned in point 4.1, catalase is the enzyme that neutralizes H_2O_2, mainly a product of photorespiration, which increases under sharp illumination. From this point of view, the increase in catalase activity indicates an adequate

response of the plants placed under the new light conditions. However, this response is likely at the cost of some compromises with the carbon budget of the saplings. The picture is similar to another crucial enzymatic antioxidant – superoxide dismutase, whose activity is highest in PP 1 and most plots, except the windward PP3, which is significantly more active in the O-plots than the C-plots. The higher activity in PP1 of this enzyme, related to ROS produced in the light phase of photosynthesis, indicates both the higher load of reactive oxygen species and the effort of saplings to cope with it under harsher conditions. Another enzymatic antioxidant – guaiacol peroxidase (GPX), is involved in phenolic synthesis and the lignification of cell walls. It also protects auxins from oxidation and rapid destruction. GPX activity is an essential indirect marker for symbiosis with arbuscular mycorrhizal fungi. Domokos et al. (2018) found more than 30% higher GPX activity in *Artemisia annua* L. plants controlled by arbuscular mycorrhizal fungi compared to the uninfected control. From this point of view, GPX is an essential antioxidant, helping plants compensate for ROS stress and maintain cell division and, therefore, growth. An increase in GPX activity relative to C-plots was observed in PP 1 (2.05 times) and especially in PP 3 (3.69 times). In contrast, in PP 2 and PP 4, the GPX levels in C-plots were comparably high with those in O-plots, which is a signal for intensive growth of saplings not only in the cut but also in the compacted parts of the forest but also probably an indirect signal for the presence of mycorrhiza in PP 1 and PP 3 (Figure 4–18).

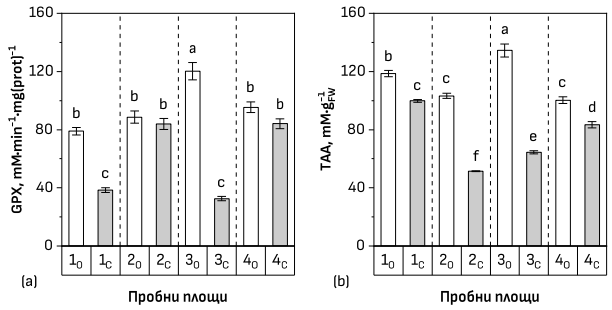

Figure 4–18. Guaiacol peroxidase (a) and total antioxidant (b) activity.

Thus, the total antioxidant activity is higher in all O-plots compared to C-plots. However, if this excess for PP 2 and PP 3 is over 2 times, then in PP 1 and PP 4, it is only about 1.2 times.

4.2.8. *C/N-balance*

In the windward PP 3_O, the carbon content in the leaves was 5% lower, and the nitrogen content was more than 11% higher than in the leaves in PP 3_C (Figure 4–19).

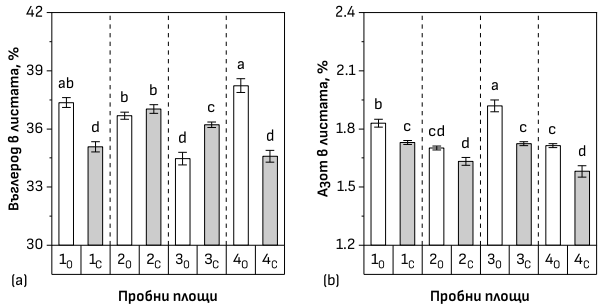

Figure 4–19. Carbon (a) and nitrogen (b) contents.

In the other test plots, where a higher nitrogen content in the O-plot leaves is observed (PP 1 and PP 4), this is also combined with more carbon, which is explained by the more intense metabolism with access to more light. In PP 2, no significant differences are observed between the nitrogen and carbon content in the leaves under the canopy and the window opened during felling. On the other hand, in PP 2, the ratio between carbon and nitrogen is one of the highest and approaches the optimal values of 24 cited in the literature. However, such levels are not reached in any test plot.

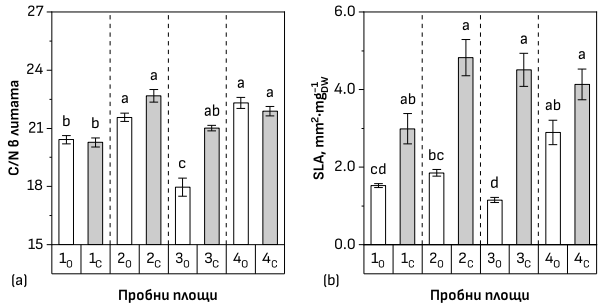

Figure 4–20. C/N-balance (a) and specific leaf area (b).

The only PP in which the balance between carbon and nitrogen is deteriorated and is lower than 18 is PP 3_O, where it is possible that the stress from the large-scale damage and the extreme change in the light, and hence in the temperature-humidity regime, have led the saplings of European beech to a state of inefficient absorption of soil resources. PP 3_O is also the sample plot where the specific leaf area (SLA) is the lowest, i.e., the leaves have a small area, a thick leaf plate and a low percentage of water content. If a lower SLA value characterizes the solar leaf ecotype, then the differences in the values of this indicator vary from 1.42 times for PP 4 through 1.95 times for PP 1, 2.61 times for PP 2 and as much as 3.92 times for PP 3.

4.3. Phenology

The plant phenological index PPI shows a specific seasonal trajectory in both sites and particular dynamics during the individual years of the study. For both sites, the maximum summer values of PPI will be reached in 2019 and 2021, while PPI will be limited to relatively lower summer maxima in 2017, 2020, and 2022. 2019 and 2021 are characterized by a warmer and drier summer (June–August) compared to 2017 and 2020. However, the most significant

difference between 2019/2021 and the other years during the study period is the precipitation amounts and temperatures during the dormant period (November–April). The dormant period of 2018–2019 and that of 2020–2021 is characterized by moderate temperatures and precipitation amounts, while in the remaining years, significant variations are observed around the norm for 2001–2020. The dormant period before 2017 and 2022 was relatively cooler and drier, especially in spring. (Figure 4–21).

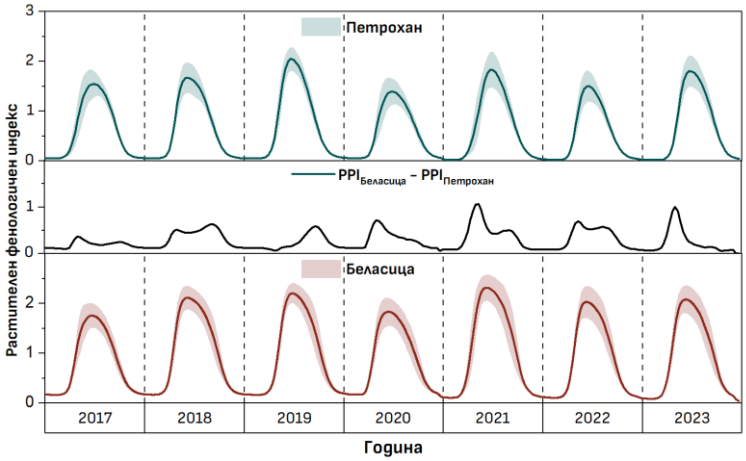

Figure 4–21. Plant phenology index in Petrohan (a) and Belasitsa (b) for 2017-2023.

The dormancy before 2018 was relatively short, and before 2020 and 2023 - it was warm, especially during the preparation period for wintering (November) and the preparation period for exiting dormancy (February–March).

4.3.2. *Start of season date*

The beginning of vegetation (SOSD) for Petrohan is, on average, on April 21 (±12.6 days standard deviation) and varies between April 12 in 2018 and April 25 in 2019 and 2023. For Belasitsa, the same indicator (SOSD) occurs on average almost on the same day – on April 22 (±11.5 days standard deviation), and here, the variation is also significant – between April 11 in 2018 and April 30 in 2023. The date of mass leafing of the European beech is subject to year-specific combinations of environmental factors. (Figure 4–22).

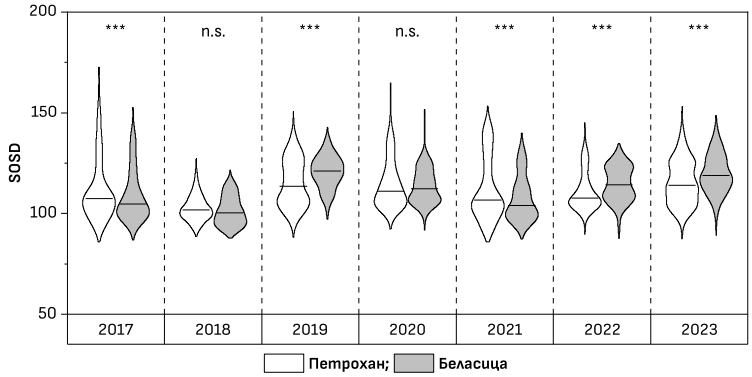

Figure 4–22. Start of season date.

In 2021, in both studied mountains, leafing begins early in the lower parts, but a sharp boundary is outlined at about 1000 m asl, which separates leafing in the higher parts for a later period. This year, after a relatively mild winter, April in the mountains is more than one and a half degrees cooler and about 150% more humid than typical. Although the appropriate light conditions have occurred (13 hours of daylight and sufficient blue light), leafing under such conditions is delayed. A sharp warming follows in May, which triggers expressive leafing above 1000 m asl. A similar but less contrasting picture is in 2017 when the boundary descends to a lower altitude. April 2012 has temperatures around the norm but comes after an icy January (3–4 °C negative anomaly in the mountains). The warming in May, although not as pronounced as in 2021, still triggers a sharp mass leafing out of a larger area. The start of the season in 2018 is impressive, when – due to the warming in March, which persisted in April and May – leafing out is expressive.

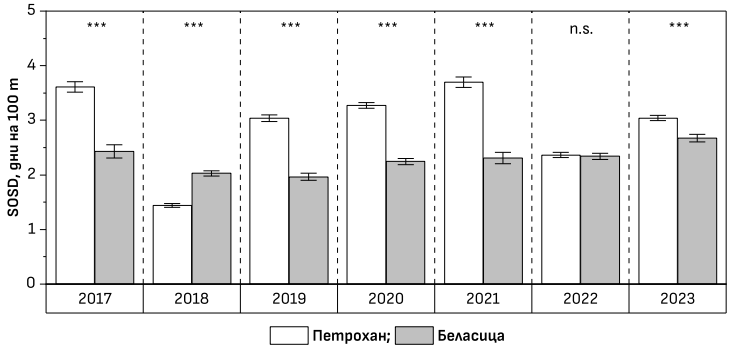

Figure 4–23. Start of season date per 100 m.

To overcome 1000 m above sea level, in which range the central massif of beech stands in both mountains are locked, it takes a little more than half a month, unlike other years, when the same range requires more than a month – for example, in 2023 when the spring is significantly cooler. For each of the years in Belasitsa, defoliation climbs in altitude by 2.3 days per 100 m with a slight variation of only SD = 0.2 days. In Petrohan, this process occurs more slowly in most years, except for 2022, when defoliation crawled along the slope with a similar speed in both sites. In 2018 (with the warmest spring) – in Petrohan, it is significantly more expressive. The average rate at which defoliation overcomes the elevation change in Petrohan is 2.9 days per 100 m, but already with a more considerable variation of SD = 0.8 days. The most extensive lag in defoliation in Petrohan, compared to Belasitsa, is observed in 2017 and 2021, when spring temperatures are lower; thus, defoliation in the more northern region is delayed. The anomaly of 2018 can be explained not only by the warmer spring in Bulgaria as a whole but also by the better moisture storage in Petrohan, where more precipitation falls in total for the four months of deep dormancy (from December 2017 to March 2018) than in Belasitsa for an entire year (any) of the study period. (Figure 4–23). In 2022 addition to the warmer than other years,

January and April, the amount of precipitation during the dormant period (the time during which moisture accumulates in the soil) was also significant.

4.3.3. *Maximum of season date*

The day of maximum greening occurs earlier in Petrohan than in Belasitsa, except in 2017, when the difference is insignificant (Figure 4–24).

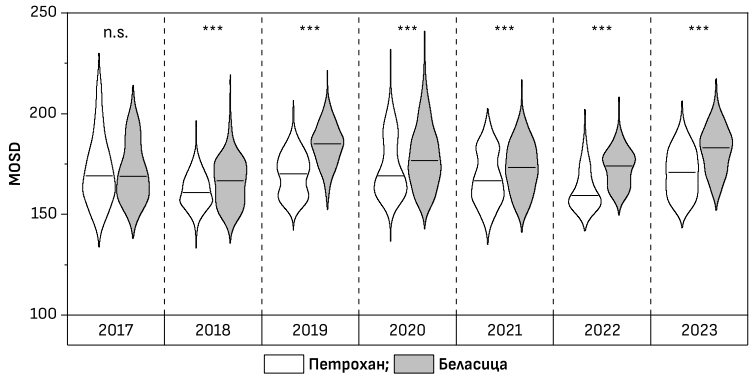

Figure 4–24. Maximum of season date (MOSD).

The average MOSD value of Petrohan is June 17 (±13.3 days), a whole week before that of Belasitsa – June 24 (±13.8 days). At Petrohan, MOSD varies between June 11 (±8.7 days) in 2018 and June 23 (±14.8 days) in 2020. For Belasitsa, this range of variation is also more extensive – from June 16 (±11.9 days) in 2018 to July 4 (±10.4 days) in 2019. The differences between the two sites are the smallest in this indicator in 2017 and the largest in 2019 and 2022 when the summer is drier and hotter.

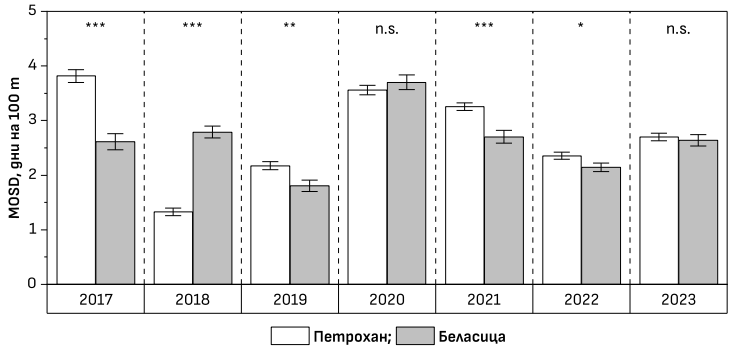

Figure 4–25. Maximum of season date (MOSD) per 100 m.

In Petrohan, MOSD creeps by 2.7 ± 0.9 days per 100 m and varies from 1.3 days in 2018 to 3.8 days in 2017. In Belasitsa, the values are similar – an average of 2.6 ± 0.6 days per 100 m and a variation between 1.8 days in 2019 and 3.7 days in 2020. The relationship of altitude with MOSD becomes more variable than that with SOSD. Although the difference between the two sites is significant in most years, MOSD in Belasitsa creeps up the slope faster than in Petrohan. The values are still significantly less different than those for SOSD (Figure 4–25).

4.3.4. *End of season date*

The autumn phenology is represented by the mass leaf browning stage – EOSD. This event occurs significantly earlier at the site located at a higher latitude – Petrohan, where it appears on average on October 15 (±10.3 days). At Belasitsa, the average leaf browning date is more than 11 days later – on October 26 (±10.4 days) (Figure 4–26).

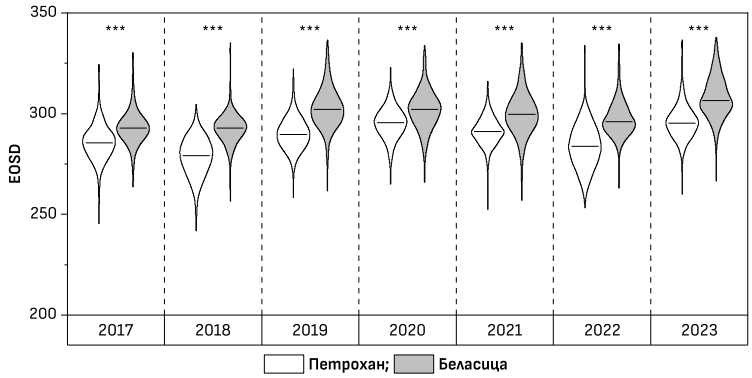

Figure 4–26. End of season date (EOSD).

Annually, this delay in the browning of beech in Belasitsa is between 6 days in 2021 and 14 days in 2018 and 2022. It is striking that the year in which leafing occurs earliest (2018) is also the year in which the leaves turn brown earliest – October 5 for Petrohan and October 19 for Belasitsa. Although the study period is short of considering significant trends, it is striking that with each passing year, the browning of the leaves occurs later and later – for Petrohan by as much as 17.2 days later (October 22), and for Belasitsa – 15.5 days later (November 4) in 2023, compared to 2018.

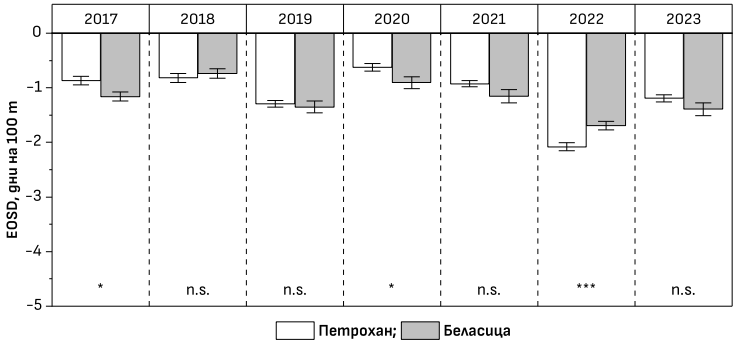

Figure 4–27. End of season date (EOSD) per 100 m.

In confirmation that the relationship between EOSD and altitude is not as strong as for SOSD, and the relationship with latitude is already strengthening, the time to overcome 100 m of elevation change by this phenological manifestation is significantly shorter. In most years, the rates at which EOSD creeps down the slope are similar at both sites and vary from a little more than half a day for 100 m of elevation change (0.6 days for Petrohan and 0.7 days for Belasitsa) in 2020 to only 2.1 days for Petrohan and 1.7 days for Belasitsa in 2022, when it is the most

significant difference between the two sites. It turns out that autumn browning of leaves occurs significantly more expressively than leaf fall (Figure 4–27).

4.3.5. *Length of season in days*

The length of the growing season (LOSD) is longer in Belasitsa (185.2 ± 14.8 days) compared to Petrohan (176.1 ± 17.3 days). For Belasitsa, this indicator varies between 180.0 ± 13.3 days in 2019 and 190.8 ± 16.2 days in 2021, and for Petrohan – between 172.0 ± 17.7 days in 2022 and 180.0 ± 16.6 days in 2020 (Figure 4–28).

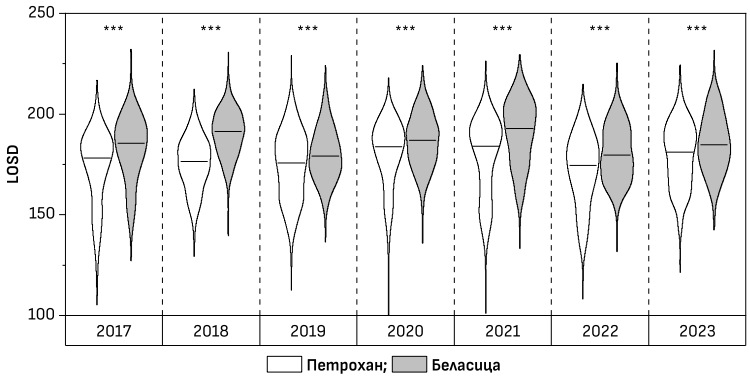

Figure 4–28. Length of season in days (LOSD).

The difference in the length of the growing season is probably due to slower leafing in spring and earlier browning in autumn in Petrohan compared to Belasitsa. It is less affected by the date of leafing in spring or the rate of browning in autumn. However, the relationship between altitude and LOSD is more substantial than with SOSD. (Figure 4–29).

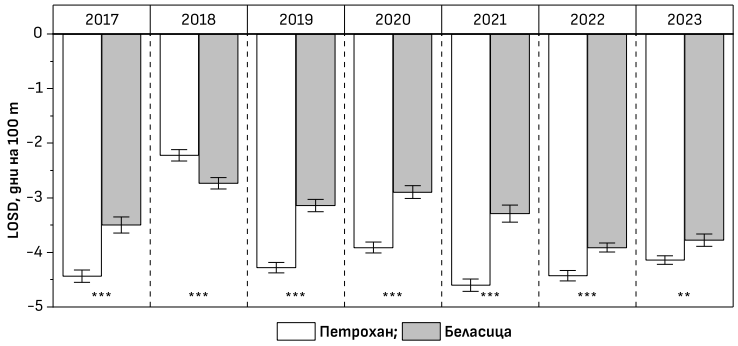

Figure 4–29. Length of season in days (LOSD) per 100 m.

The growing season is shortened by an average of 4.0 ± 0.8 days with a 100 m elevation increase in Petrohan and by 3.3 ± 0.4 days in Belasitsa. Except for 2018, when both spring and autumn phenological events in Petrohan are significantly more expressive, leading to a weakening of the relationship with altitude, in all other years, the change in LOSD with altitude change here is more significant than in Belasitsa.

4.3.6. *Discussion*

The difference in latitude between the two studied sites (<2°) affects the phenological manifestations of European beech, although not always unambiguously. Against the background of the similar trend in the seasonal trajectories of the plant phenological index, its maximum levels are reached at different optimal temperatures, which differ approximately as much as the difference in the average temperatures in the two sites. When indexing the temperatures as a percentage of the annual amplitude, the differences between the two sites are blurred, and the maximum value of the vegetation phenological index is reached at similar (~88% of the annual amplitude) relative temperatures. Such blurring of the differences between the two sites, different in hydro-thermal terms and at a significant distance in terms of their latitude, indicates a preserved potential for adaptation of the species to the climatic features in the mountains of Western Bulgaria. In 2018, leafing occurs early – already in the first half of April, with the prerequisites related to a mild winter – January, February, and March have a 1.5 °C positive anomaly. This is followed by significant warming in April, when Petrohan recorded an average monthly temperature of 9.7 °C, compared to the 1961–1990 norm of only 3.9 °C. At the same time, February and March have doubled the amount of precipitation in most of the country, and in the mountains, this excess is more than twice. Some authors (Peaucelle et al. 2019) found that earlier leafing is mainly influenced by the daytime temperature, with a decrease in response to weaker cooling compared to daytime warming observed in recent years. The annual specificity, which is established in the seasonal trajectories of the plant phenological index, is probably due to specific conditions in the preceding vegetation and the dormant period and not to spring forcing. Such a tendency may be related to the particular strategy of European beech, which is to invest significant resources and time in bud formation during winter. Roberts et al. (2015) found that European beech is less sensitive to spring forcing than other European tree species and pointed to the role of dormancy induction in spring phenology. Badeck et al. (2004) pointed out that annual variations in the timing of phenological events in some tree species can reach up to one month.

On the other hand, Vitasse & Basler (2013) found that the bud break date of European beech shows less temporal and spatial variation than most other broadleaf tree species in Europe, which the late leafing of this species can explain, which is probably the reason for the more minor differences between the two sites we found in SOSD compared to MOSD and even more so in EOSD. We did not find significant differences in SOSD between the two sites after a dry and warm dormant period (November–April), while the most considerable differences in this indicator were found after a wetter and cooler dormant period that delayed leafing in the more

southern Belasitsa. The most significant differences in MOSD between the two sites were found after a drier spring (March–June), explaining the earlier depletion of the potential for PPI to increase in Petrohan. The forests in Belasitsa, better adapted to lower precipitation, are less sensitive to this stressor. EOSD is the phenological indicator with the most significant differences between the two sites. Vegetation in Belasitsa ends 1–2 weeks later than in Petrohan, probably due to higher temperatures and lower precipitation in autumn. The early onset of EOSD in 2018 and 2022 in both locations occurs against the backdrop of a very dry October, and the late onset of this phase occurs during the relatively warmer and wetter autumns of 2019 and 2023. Contrary to the prediction of Roberts et al. (2015), we did not observe a significant temporal shift in SOSD or other phenological events, likely due to the short study period.

Some authors (Petkova-Tsokova 2019) point out that the phenological phases of beech are, to a greater extent, genetically predetermined and, to a lesser extent, influenced by changing environmental conditions. Such a tendency can be seen as a sign of an adaptation of the species during evolution, but it speaks of a more conservative acclimation approach. The adaptation to local conditions is also supported by the established better height growth for local origins, compared to Central European ones in Bulgaria's warmer and drier climate (Petkova-Tsokova 2019). Contrary to the trend in the differences in the average dates of phenological events occurring in the two places, the speed with which these events occur with a change in altitude is more noticeable in spring. In Petrohan, it takes more than 38 days for the European beech to leaf out to overcome 1300 m above sea level; in Belasica, it takes 10 days less for almost the exact elevation change. Similar results were reported by Čufar et al. (2012) for Slovenia, where the rate of leafing out is 2.6 days per 100 m elevation change. Schieber et al. (2013) found between 2.83 and 3.00 days of spring phenology shift per 100 m elevation change in the Western Carpathians in Slovakia (~49°N). Dittmar & Elling (2005) found a shift of as much as two days per 100 m faster in the start of vegetation in southern Bavaria (Northern Alps and Bavarian Forest) compared to the northern regions of Bavaria, which they explained by unfavourable heat and radiation conditions in the north. The differences are weaker for MOSD, and for EOSD, they even become insignificant in most years. Suppose spring phenological events occur slowly at different altitudes. In that case, it is clear that later phenological events are significantly less related to this factor, and the role of latitude comes to the fore. Only in 2022 do we report a more significant influence of altitude on EOSD (2.1 days per 100 m at Petrohan and 1.7 days per 100 m at Belasitsa). 2022 is also the year with the shortest growing season during the study period. Despite slight variations in individual years, the growing season

is shorter at higher altitudes and much more pronounced in Petrohan than in Belasitsa. Urban et al. (2015) indicate leaf browning starts later at higher temperatures, but leafing is less sensitive to elevated temperatures.

The phenology of European beech is closely related to the factors of latitude and altitude. Spring phenological events show a stronger relationship with altitude than with latitude. In summer, this relationship weakens, and in autumn, latitude emerges as a limiting factor. Although the end of the season occurs later with each passing year, the relationship is still insignificant, probably due to the short period of the study. The dynamics of individual phenological events in different years, at various altitudes and other latitudes, is a marker for a good potential for acclimation of European beech to the modern climatic conditions in Western Bulgaria. Moreover, for geographical crops, Petkova-Tsokova (2019) found that the date of leafing out is directly proportional to longitude, i.e. moving the origins to the east leads to earlier leafing out. She also points out that autumn leaf colouring is inversely proportional to longitude but directly proportional to latitude, i.e. in eastern and southern origins, autumn phenophases occur later.

4.4. Natural disturbances

4.4.1. *Vegetation indices dynamic in 2017 – 2023*

Images captured between July 15 and August 15 were downloaded for four years (2017, 2019, 2021 and 2023) for three vegetation indices to assess the damage caused by ice break. By definition, NDVI ranges from -1 to 1. Negative values are characteristic of inanimate objects – rocks, water bodies, etc. It is noteworthy, however, that NDVI saturates with values above 0.6. Therefore, the range of variation is presented on the maps only for positive levels of the index (0-1), characteristic of living plants. However, no significant differences are observed between individual years, including the year of the ice storm 2021. Such tendency is also evident from the average value for the image from August 1 of the year of the natural disturbance – 0.855 ± 0.054, which, although significantly different from those in other years, is much smaller in percentage terms compared to the other indices.

Table 4–1. Vegetation indices dynamic in 2017 – 2023. The second row showed the index as a % of 2021.

Vegetation indices	2017	2019	2021	2023
NDVI	0.886±0.045 b 103.6%	0.889±0.038 a 104.0%	0.855±0.054 d 100%	0.858±0.041 c 100.4%
LAI	3.956±0.854 a 110.3%	3.898±0.840 b 108.7%	3.587±0.888 d 100%	3.710±0.790 c 103.4%
PPI	1.473±0.548 a 111.8%	1.402±0.496 c 106.3%	1.318±0.502 d 100%	1.468±0.516 b 111.4%

The values shown in Table 4–1 show that the dynamics of NDVI are the smallest, which means that this index can be defined as weakly sensitive to changes caused by natural disturbances.

Other authors obtained similar results (Nedkov et al. 2020) who used NDVI to assess damage from natural disturbances. On the other hand, PPI is the most sensitive of the studied indices, at least as far as the percentage ratio to the average value in the year of the ice storm is concerned. It is striking, however, that there is a considerable difference between the pre-icebreaker years of 2017 and 2019, which cannot be explained by larger-scale disasters in this period. Also, PPI has already recovered to close to maximum levels in 2021, i.e. two years after the icebreaker, which indicates that the index is susceptible to green vegetation, regardless of whether it is in the grass, shrub or tree horizon of the vegetation cover, which is also confirmed by the analysis of the generated difference images - 2019-2017, 2021-2019 and 2023-2021 for the three studied indices.

The NDVI difference images show noise with no biological explanation but are more likely due to distortion in the Sen2Cor procedure on the https://wekeo.eu servers. Here, PPI has the fewest invalid pixels (barely 3.4%, compared to more than 11% for NDVI and 6.2% for LAI). However, in the 2021-2019 difference, probably due to the wetter winter and spring of 2021, positive values (indicated by arrows) are observed in the range outside the damaged area (above 1000 and below 500 m asl), which broadly neutralize the negative values in the icebreaker zone. Thus, the average difference PPI value for the 2021-2019 image is similar to that of the previous difference period (2019-2017). Such a tendency confirms the choice of the leaf area index (LAI) as the most appropriate of the considered indices in assessing the extent of ice storm damage in 2021. Another positive aspect of LAI is that this index is well known in global forestry science, it has a direct (and linear) relationship with forest productivity (Clark et al. 2008), at least in the range LAI = 0 – 5.

By the beginning of June 2021, signal sheets for established damages in 148 stands were submitted to the Berkovitsa Regional Directorate. The presented LAI difference map for 2021-2019 shows that the territory most severely affected by the icebreaker has been bypassed, and the established damages have been signalled. However, there are still stands in which damages are visible on satellite images but are not described in signal sheets, probably due to their more inaccessible nature or the too voluminous and challenging task of explaining the many objects. Similar is the case with stands 37c, 15h, 16d, and 17f in the Prazhkovitsa region, as well as 183b, 183c, 186a, 187 a, 188a, 209c, 218p and others. It should be noted, however, that the description of the damage caused by the icebreaker was not completed by 01.06.2021. In addition, the LAI difference map shows damage and stands expressed in the refraction of the crowns, most often the tops, which causes a reduction in LAI. On the other hand, signal sheets have been submitted for some stands in which the damage is only in a limited area and not on

the territory of the entire stand – 47c, 48b, 178c, 180b, 180c, 204h, etc., which is visible on the difference map.

4.4.2. *Assessment of risk factors for ice break damage*

The generated difference map can be used to extract information about the extent of damage – in absolute terms (as the difference between the LAI of 2021 and the LAI of 2019) or in relative terms (as the ratio between the LAI of 2021 and the LAI of 2019). In both cases, the convenience is that this information can be compared with forest inventory and physical characteristics of the stands to analyze available relationships. The analysis shows that all average values of $\Delta LAI_{2021\text{-}2019}$ for altitudes below 550 m and above 1100 m do not differ significantly from zero. In the range from 550 to 1100 m, there is a gradient of damage, which is greatest at 900 m and smoothly decreases with increasing and decreasing altitude. It is likely that below 550 m the air temperature was around and above freezing and the rain that caused the event did not permanently turn into snow to accumulate and cause damage.

On the other hand, above 900 m, the damage decreases rapidly and above 1100 m, there were probably no conditions for snow accumulation and icing of the stems and crowns because the temperature was already low enough for the snow not to be retained by the crowns, which is also why only the stand with an altitude between 550 and 1100 m were filtered in the analysis. Of these, only the stands in which $\Delta LAI_{2021\text{-}2019}$ is significantly less than zero (T-test, P-value < 0.05) were filtered.

The total number of stands for which these conditions are met is 745, which does not mean that these are the only stands with icebreaker damage and also does not mean that in each of these stands, the damage was of such magnitude as to justify submitting a signal sheet to the RDG. Moreover, the most number of stands is in the range LAI = [-0.5 ÷ 0] – 288 units, followed by those in which the damage is in the range $\Delta LAI_{2021\text{-}2019}$ = [-1.0 ÷ -0.5] – 257 units, those in which the damage is in the range $\Delta LAI_{2021\text{-}2019}$ = [-1.5 ÷ -1.0] – 117 units, those in which the damage is in the range $\Delta LAI_{2021\text{-}2019}$ = [-2.0 ÷ -1.5] – 53 units, those in which the damage is in the range $\Delta LAI_{2021\text{-}2019}$ = [-2.5 ÷ -2.0] – 26 units and only four stands have damage of $\Delta LAI_{2021\text{-}2019}$ = [-3.5 ÷ -2.5]. Damage is concentrated in stands at 900 m above sea level. At this altitude, there are individual stands where the reduction in leaf area is almost 3 m2, which in a mature or maturing beech stand may be the entire LAI. At 1100 m, the average damage is already only -0.394±0.064, which is most often expressed in broken branches of individual trees. (Figure 4–30).

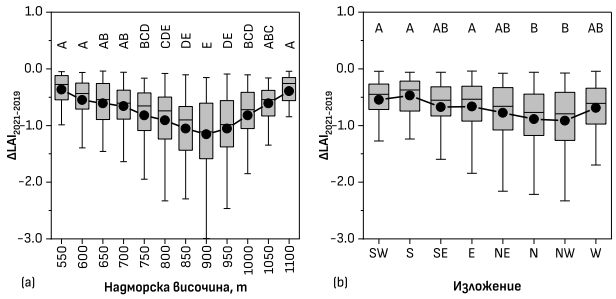

Figure 4–30. $\Delta LAI_{2021-2019}$ as relation to altitude (a) and aspects (b) of damaged stands.

Regarding the distribution of damage, depending on the exposure of the stand, the most severely affected were the stands with northwest and north exposure, and the least severely affected were those with south and southwest exposure. Here, the variation between individual exposures is significantly smaller ($F = 5.82$, P-value < 0.001) compared to that between individual altitudes ($F = 14.62$, P-value < 0.001). The most severely affected are the broadleaf tall-stem forests, in which $\Delta LAI_{2021-2019} = -0.90 \pm 0.03$, while the conversion forests and coniferous forests have significantly less damage (Figure 4–31).

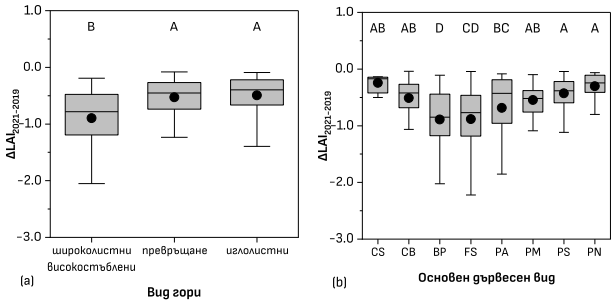

Figure 4–31. $\Delta LAI_{2021-2019}$ as relation to type of forests (a) and dominant tree species (b) of damaged stands.

Of the broadleaf species, the greatest damage is in stands dominated by European beech ($\Delta LAI_{2021-2019} = -0.883 \pm 0.025$) and birch ($\Delta LAI_{2021-2019} = -0.889 \pm 0.108$). The stands dominated by European hornbeam ($\Delta LAI_{2021-2019} = -0.513 \pm 0.051$) are slightly less damaged, and the least damaged are those dominated by common chestnut ($\Delta LAI_{2021-2019} = -0.245 \pm 0.173$). For comparison, with coniferous species, it is unsurprising that with their superficial root system, the greatest damage is in stands dominated by Norway spruce ($\Delta LAI_{2021-2019} = -0.686 \pm 0.099$). The Douglas fir crops were slightly less damaged ($\Delta LAI_{2021-2019} = -0.545 \pm 0.052$), and the least damaged were the Scots pine plantations ($\Delta LAI_{2021-2019} = -0.427 \pm 0.030$) and Austrian pine plantations ($\Delta LAI_{2021-2019} = -0.305 \pm 0.057$). However, in stands with the main tree species, European beech, the most extensive damage was also observed - in three of the four stands with $\Delta LAI_{2021-2019} < -2.5$, European beech had a share of 1, and in the fourth - 0.9, in a mixture with spruce - 0.1.

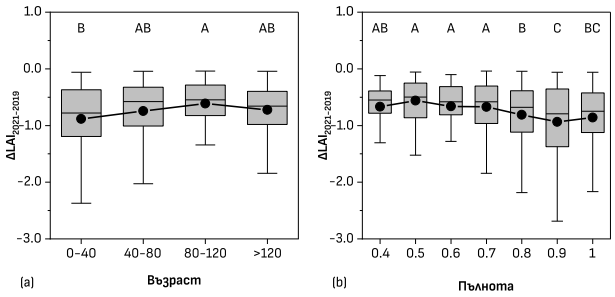

Figure 4–32. $\Delta LAI_{2021-2019}$ in relation to age (a) and stand density (b) of damaged stands.

Regarding the age at which the damage was most significant, although the two most severely affected stands were 60 years old, the damage was greatest in the young forest group – from 0 to 40 years old, and the least affected were the forests in the age group from 80 to 100 years old (Figure 4–32). High completeness (above 0.8) is associated with greater damage, while stands with completeness between 0.5 and 0.7 are the least affected. Three of the four most severely affected stands had a completeness of 0.9, and the fourth – a completeness of 0.8. The most affected were stands that developed on "brown transitional" soil, and the least affected were those on "grey forest" soil. In terms of depth – the riskiest is the deep soil, and the least dangerous is the medium-deep one. Such a tendency can be explained by the tendency of trees on poorer and shallower soils to invest in more powerful root systems to more effectively seek the resources supplied by the soil - water and minerals.

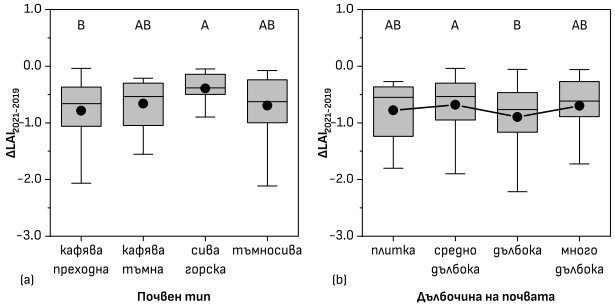

Figure 4–33. $\Delta LAI_{2021-2019}$ in relation to soil type (a) and soil depth (b) of damaged stands.

At the same time, such an investment is not required on deeper and richer soils, and resources are directed to aboveground biomass. Thus, the aboveground/belowground biomass ratio is unfavourably large in deeper, water- and mineral-rich soils. Forests on steep and very steep terrain are more severely damaged, while those on flat and sloping terrain have less damage. The four severely damaged stands with $\Delta LAI_{2021-2019} < -2.5$ have terrain slopes from 17 to 24°. Although the variation is minor ($F = 4.087$, P-value = 0.007), state-owned forests and those of legal entities are still more severely damaged compared to private and mainly municipal forests (Figure 4–34).

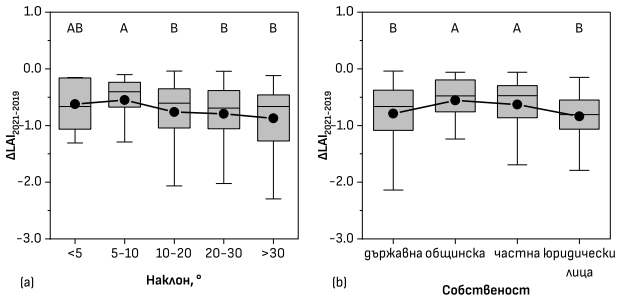

Figure 4–34. $\Delta LAI_{2021-2019}$ in relation to slope (a) and the property (b) of damaged stands.

Surprisingly, forests that were initially in poor condition did not differ in the extent of damage from forests in average and even good condition (Figure 4–35). Even the four most severely damaged stands with $\Delta LAI_{2021-2019} < -2.5$ were in the group of forests in good condition.

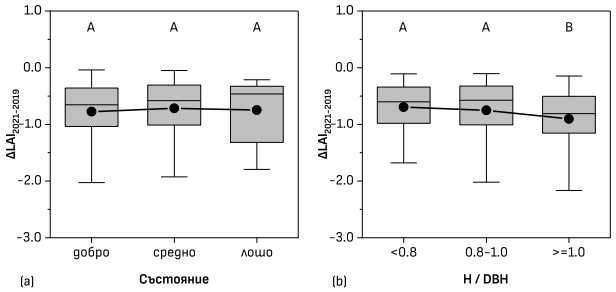

Figure 4–35. $\Delta LAI_{2021-2019}$ in relation to condition (a) and H / DBH index (b) of damaged stands.

Not surprisingly, however, is the following relationship – that of the extent of damage and the mechanical resistance coefficient of the stands, calculated as the ratio between the height and the average diameter of the stand. The most severely damaged stands are those in which this ratio is greater than or equal to 1.0, as were three of the four most severely damaged stands with $\Delta LAI_{2021-2019} < -2.5$. From the data presented, it follows that the typical profile of the damaged stands is a state forest at about 900 m, with a north-westerly exposure, with a predominance of European beech about 40 years old, with a fullness of 0.9, growing on deep, brown transitional soil and not cultivated in time to increase the H / DBH ratio above 1.0.

4.4.3. *Restoration of the territory*

Two of the four most severely damaged stands with $\Delta LAI_{2021-2019} < -2.5$ are in stand 147, letters “d” and “e”, which are in the easement strip along the main road 81 - Sofia - Vidin. The two stands were very dense and had planned maintenance felling, which was not carried out. The height of the trees was 20 m, and the diameter at breast height - 20 and 22 cm, respectively. The high density and weakened mechanical resistance, combined with the chance of being in the path of the storm, are the basis of the significant damage, more pronounced in the lower part of the stand bordering the road, which is also steeper. NDVI stands out as a more conservative index. There is no reliable difference between the index for 2017 and 2019 but after the drastic damage from the icebreaker in 2021. NDVI decreases by just over 30% to

0.62±0.01, which is categorized as a “mild stress” level in most NDVI studies. PPI is more dynamic, and in addition to the significant difference between the 2017 and 2019 indices, the decrease in PPI in 2021 compared to 2019 is as much as 73% to 0.49±0.01. However, in 2023, the PPI recovers to 67% of the 2019 value of 1.22±0.03, which is already a significantly high value with a PPI range between 0 and 3 and a maximum value for the period of 1.82±0.04 in 2019 (Figure 4–36).

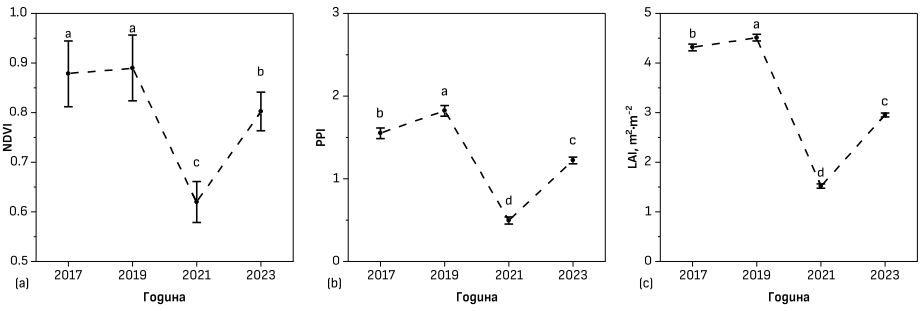

Figure 4–36. Dynamics of vegetation indices in most damaged stand 147.

And when assessing recovery, LAI emerges as the most relevant of the studied indices. Its value decreases by 67% after the icebreaker to 1.52±0.04 in 2021, compared to 2019, and in 2023, it recovers to 2.95±0.04, with a range of variation from 0 to 7 and a maximum value for the period of 4.51±0.07 in 2019.

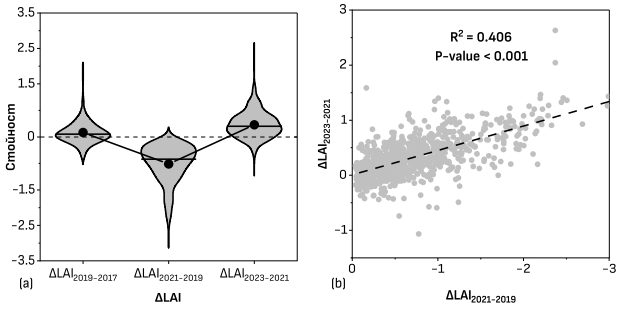

Figure 4–37. Leaf area index (LAI) in damaged stands.

The average LAI change for 2017–2019 – $\Delta LAI_{2019\text{-}2017}$ = 0.123±0.012 is significantly higher than zero (T-test, P-value < 0.001). As a result of the icebreaker, the change in LAI for the period 2021-2019 is in a negative direction – $\Delta LAI_{2021\text{-}2019}$ = 0.762±0.020, with more than 4% of the affected stands having $\Delta LAI_{2021\text{-}2019}$ < -2.0, 11.1% having $\Delta LAI_{2021\text{-}2019}$ < -1.5 and 26.8% having $\Delta LAI_{2021\text{-}2019}$ < -1.0. In the initial stages of the succession, the recovery of LAI proceeds slowly, and in the period 2021-2023, only 0.2% of the affected stands have $\Delta LAI_{2023\text{-}2021}$ > 2.0, and only 5.1% of the stands have $\Delta LAI_{2023\text{-}2021}$ > 1.0. LAI is still decreasing for some stands, possibly due to the continued utilization of damaged wood or the deterioration of stands with damaged crowns. As many as 17.5% of the affected stands have $\Delta LAI_{2023\text{-}2021}$ < 0.0. However, the correlation between the extent of damage (in $\Delta LAI_{2021\text{-}2019}$) and the rate of LAI recovery (in $\Delta LAI_{2023\text{-}2021}$) for the affected area is quite clear. The Pearson coefficient is -0.673, and R2 = 0.406, with a P-value < 0.001, which shows that despite the large extent of the damage, the fact

that the most severely damaged stands have a shady exposure (NW and N) leads to their rapid grassing, and this significantly limits erosion from the cleared forest area.

4.4.4. *Response of saplings to canopy opening*

In June 2024, physiological indicators were measured in some of the stands most severely affected by the ice storm. Exact measurements were also carried out in less affected stands to compare the results of these saplings.

Table 4–2. Stands and LAI dynamics.

Stand	Altitude, m	$\Delta LAI_{2019-2017}$	$\Delta LAI_{2021-2019}$	$\Delta LAI_{2023-2021}$
147e	900	0.197±0.029	-2.993±0.065	1.432±0.044
20в	950	0.360±0.010	-1.883±0.032	0.975±0.019
155д	700	0.086±0.042	-0.859±0.066	0.300±0.054
143б	1000	0.072±0.024	-0.609±0.034	0.315±0.020

The constructed light curves of photosynthesis show the species' plasticity to the environment's light conditions. In the most severely affected stand 147e, the variations of photosynthesis at individual light levels are the greatest. (Figure 4–38).

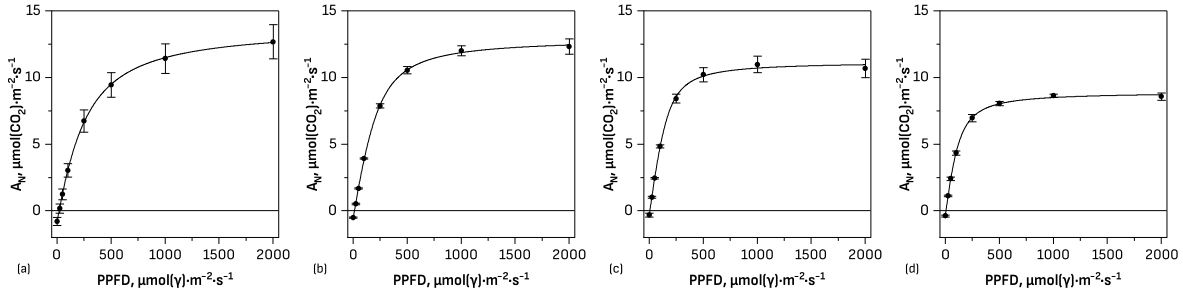

Figure 4–38. Photosynthetic light-curves of saplings in stands (a) 147e, (b) 20в, (c) 155д и (d) 143б.

The saplings' leaves reached the highest maximum photosynthesis A_{MAX} among the other sub-compartments. The respiration (R_D) of the saplings in this sub-compartment was also the most intense, resulting in the lowest light use efficiency (LUE) and the most expansive transition zone θ. The light compensation point (LCP) was the highest, as was the light saturation of photosynthesis (LSP). These results indicate the high degree of acclimation to intense light (PPFD = 1014.53 ± 89.13 µmol(γ)·m^{-2}·s^{-1}) in the sub-compartment after the large-scale damage. Although limited in number and in sharp competition with grass species and more pioneer tree species such as aspen, European ash, Douglas-fir, sycamore maple and Norway maple, which have already settled in the area stripped of the main stand, the saplings of European beech have responded adequately to the changed light regime and have formed a sunny leaf ecotype. In stand 20c, A_{MAX} decreases, compared to that in 147e. R_D, although lower in value, this difference is not significant, as are the differences in LUE. However, LCP and LSP are lower, and the transition zone is narrower.

Table 4–3. Photosynthetic light-curves parameters and relation with $\Delta LAI_{2021-2019}$.

	147e	20в	155д	143б	R
A_{MAX}	13.82 ± 0.15 a	12.94 ± 0.17 b	11.19 ± 0.22 c	8.92 ± 0.10 d	-0.913*
R_D	0.85 ± 0.07 a	0.57 ± 0.11 ab	0.33 ± 0.20 b	0.35 ± 0.10 b	-0.989**
LUE	0.047 ± 0.002 b	0.049 ± 0.003 b	0.059 ± 0.006 ab	0.061 ± 0.004 a	0.955**
θ	0.473 ± 0.056 b	0.744 ± 0.047 a	0.810 ± 0.062 a	0.717 ± 0.052 a	-0.838n.s.
LCP	18.93 ± 1.06 a	11.70 ± 1.89 b	5.59 ± 2.99 c	5.74 ± 1.37 c	-0.993***
LSP	1136.94 ± 68.80 a	597.05 ± 49.85 b	354.03 ± 47.23 c	346.82 ± 29.65 c	-0.975**
PPFD	1014.53 ± 89.13 a	331.59 ± 53.80 b	89.77 ± 13.30 c	13.6 ± 1.53 d	-0.974**

These characteristics indicate light acclimation, which is not as strong as in the saplings in stand 147e. Still, the illumination (PPFD = 331.59 ± 53.80 $\mu mol(\gamma) \cdot m^{-2} \cdot s^{-1}$) in this stand is about three times lower. The leaf petiole is no longer as small and leathery as in 147e. In stand 155e, there is only one fallen stem from an icebreaker, but the crowns of most adult trees are significantly damaged. This results in a luminosity PPFD = 89.77 ± 13.30 $\mu mol(\gamma) \cdot m^{-2} \cdot s^{-1}$, which – although lower than the severely affected sub-sections 147e and 20c – is significantly higher than the very slightly affected sub-section 143b, where the PPFD is only 2.4 times higher than the LCP of the saplings there. The leaves of the saplings in 155e and especially those in 143b are of a strongly shaded ecotype. The low R_D, high LUE, narrow zone θ, and low LSP confirm this. However, the physiological indices A_{MAX} and LCP are higher in the more severely affected 155e, which may be a sign that these are the first signs of light acclimation evident in the saplings‘ leaves.

CONCLUSIONS AND RECOMMENDATIONS

Conclusions

1) Populations of European beech in the studied areas possess a rich set of mechanisms for acclimation to varying environmental factors.

2) European beech can compensate for the attack of the beech leafhopper both by activating its defence system of enzymatic antioxidants and secondary metabolites and by increasing the physiological activity of the healthy part of the leaf petioles, which is possible when the carbon balance allows resources to be allocated for the defence system from the products produced during photosynthesis. Such mechanisms are used to a limited extent in a tense carbon balance.

3) Biochemical mechanisms for light acclimation of European beech saplings after opening the canopy, although they are a powerful tool for counteracting the initial stress caused by sudden illumination, often have a multidirectional nature. As a fine-tuning of acclimation, they do not affect the long-term adaptive characteristics of individuals. On the other hand, the formation of a sunny leaf ecotype ensures more stable physiological acclimation, allowing the maintenance of a carbon and water balance consistent with the changed light and hydrothermal conditions.

4) Spring phenological manifestations in European beech are more strongly dependent on altitude and autumn ones – on latitude. Such a strategy may prove favourable for adaptation to the shift of the leading snow period in late winter and early spring, as well as the increasingly long dry periods in summer and autumn.

5) European beech periodically suffers significant abiotic damage due to its shallow root system. The main risk factors associated with forest management are the weakening of mechanical resistance in uncultivated middle-aged and maturing forests and the maintenance of forests homogeneous in composition and age.

6) Although, due to the nature of its reproductive organs, the European beech has more difficulty returning to the territory affected by natural disturbance, its saplings show significant physiological plasticity and quickly acclimatize their leaf apparatus for the most effective absorption of the changed resources of the environment, even in competition with more pioneering plant species.

Recommendations

1) The successful acclimation and adaptation of the European beech to the increasingly dynamic environmental conditions should also include the adaptation of silvicultural approaches to the management of beech forests. The focus of this long-term management should be redirected from the value of the extracted resource to the vital qualities of the individuals remaining on the stand at each stage of forest development.

2) After a scientifically based analysis of the risk factors, the priority in the implementation in beech forests should be silvicultural activities that increase and maintain biological and mechanical resistance and the potential for adequate adaptation to the changing climate.

3) Thanks to remote sensing, efforts could be saved, and omissions and errors in the field assessment of natural disturbances in the forests could be avoided. This allows emergency actions to be concentrated in priority areas where damage would significantly increase the risk of fire, erosion, disaster, material losses, etc.

4) When using vegetation indices determined by remote sensing methods, the special Plant Phenology Index should be used to assess phenological development and the Leaf Area Index to assess damage from natural disturbances.

CONTRIBUTIONS

A. Scientific

1) The acclimation of the European beech was studied from the biochemical, physiological, and anatomical-morphological to the phenological level, and a logical relationship between the individual levels was sought.

2) Modern equipment and methods were used to assess the European beech's acclimation potential to the dynamics of environmental factors exacerbated by climate change, insect pests, and human activity.

3) Significant potential for biochemical and physiological counteraction to the attack by beech gall midge has been identified, provided sufficient resources are available for redistribution to defence mechanisms and compensation.

4) The relatively rapid anatomical and morphological acclimation of European beech leaves after opening the canopy has been confirmed. This allows for effective utilization of environmental resources through changes at the biochemical and physiological levels.

5) A relatively new and specially developed for phenological observations vegetation index – Plant Phenology Index – was used to track phenological development.

6) A stronger relationship was found between spring phenological events and altitude and between autumn phenological events and latitude.

Б. Applied

1) The widely accepted and applied global forest practice – leaf area index, determined through remote sensing methods, was used to assess the damage from a natural disturbance in beech forests.

2) The main risk factors for abiotic damage in beech forests due to natural disturbance have been assessed and identified.

3) A strong correlation was established between the extent of damage, calculated using remote sensing methods, and the change in physiological indicators of beech saplings in the affected stands.

4) A rich methodology has been proposed for studying the physiological acclimation of forest tree species to dynamic changes in the conditions of existence.

BIBLIOGRAPHY

Димитрова-Матева П. (2008). *Листоминиращи насекоми по обикновения бук (Fagus sylvatica L.) в Западна България* [Дисертация за ОНС "Доктор", Лесотехнически университет]. София. 131 стр.

Петкова-Цокова К. (2019). *Потенциал за приспособимост на произходи от дугласка и обикновен бук към промени в климата* [Дисертация за НС "доктор на науките", Лесотехнически университет]. София. 199 стр.

Ač A., Malenovský Z., Olejníčková J., Gallé A., Rascher U., Mohammed G. (2015). Meta-analysis assessing potential of steady-state chlorophyll fluorescence for remote sensing detection of plant water, temperature and nitrogen stress. *Remote Sensing of Environment*, *168*, 420-436.

Adamidis G.C., Varsamis G., Tsiripidis I., Dimitrakopoulos P.G., Papageorgiou A.C. (2021). Patterns of Leaf Morphological Traits of Beech (Fagus sylvatica L.) along an Altitudinal Gradient. *Forests*, *12*(10).

Aebi H. (1984). [13] Catalase in vitro *Methods in enzymology* (Vol. 105, 121-126). Academic Press.

Anev S., Dimitrova-Mateva P., Lamlom S., Chaneva G., Tzvetkova N. (2016). Non-destructive allometric method for estimation of leaf area in European beech (*Fagus sylvatica* L.). *Foresry Ideas*, *22*(2), 198–205.

Anev S., Georgieva S., Dimitrova-Mateva P., Chaneva G. (2015). Effect of beech weevil (*Orchestes fagi* L.) infestation on photosynthesis and water regime of European beech (*Fagus sylvatica* L.) leaves. *Journal of Bioscience and Biotechnology*, *special edition*, 235–238.

Arnon D.I. (1949). Copper Enzymes in Isolated Chloroplasts. Polyphenoloxidase in Beta Vulgaris. *Plant Physiology*, *24*(1), 1-15.

Badeck F.-W., Bondeau A., Böttcher K., Doktor D., Lucht W., Schaber J., Sitch S. (2004). Responses of spring phenology to climate change. *New Phytologist*, *162*(2), 295-309.

Beauchamp C., Fridovich I. (1971). Superoxide dismutase: Improved assays and an assay applicable to acrylamide gels. *Analytical Biochemistry*, *44*(1), 276-287.

Beck P.S.A., Atzberger C., Høgda K.A., Johansen B., Skidmore A.K. (2006). Improved monitoring of vegetation dynamics at very high latitudes: A new method using MODIS NDVI. *Remote Sensing of Environment*, *100*(3), 321-334.

Čater M. (2021). Response and mortality of beech, fir, spruce and sycamore to rapid light exposure after large-scale disturbance. *Forest Ecology and Management*, *498*, 119554.

Čater M., Levanič T. (2013). Response of Fagus sylvatica L. and Abies alba Mill. in different silvicultural systems of the high Dinaric karst. *Forest Ecology and Management*, *289*, 278-288.

Chang C.C., Yang M.H., Wen H.M., Chern J.C. (2020). Estimation of total flavonoid content in propolis by two complementary colometric methods. *Journal of Food and Drug Analysis*, *10*(3).

Clark D.B., Olivas P.C., Oberbauer S.F., Clark D.A., Ryan M.G. (2008). First direct landscape-scale measurement of tropical rain forest Leaf Area Index, a key driver of global primary productivity. *Ecology Letters*, *11*(2), 163–172.

Čufar K., De Luis M., Saz M.A., Črepinšek Z., Kajfež-Bogataj L. (2012). Temporal shifts in leaf phenology of beech (*Fagus sylvatica*) depend on elevation. *Trees*, *26*(4), 1091-1100.

Dittmar C., Elling W. (2005). Phenological phases of European beech (*Fagus sylvatica* L.) and their dependence on region and altitude in Southern Germany. *European Journal of Forest Research*, *125*(2), 181-188.

Domokos E., Jakab-Farkas L., Darko B., Biro-Janka B., Mara G., Albert C., Balog A. (2018). Increase in *Artemisia annua* plant biomass artemisinin content and guaiacol peroxidase activity using the arbuscular mycorrhizal fungus rhizophagus irregularis. *Frontiers in Plant Science*, *9*, 478.

Evans J.R., Santiago L.S. (2014). PrometheusWiki Gold Leaf Protocol: gas exchange using LI-COR 6400. *Funct Plant Biol*, *41*(3), 223-226.

Fischer A. (1994). A model for the seasonal variations of vegetation indices in coarse resolution data and its inversion to extract crop parameters. *Remote Sensing of Environment*, *48*(2), 220-230.

Genty B., Briantais J.-M., Baker N.R. (1989). The relationship between the quantum yield of photosynthetic electron transport and quenching of chlorophyll fluorescence. *Biochimica et Biophysica Acta (BBA) - General Subjects*, *990*(1), 87-92.

Hart M.A., Tyson H., Bloomberg R. (1971). Measurement of activity of peroxidase isoenzymes in flax (*Linum usitatissimum*). *Canadian Journal of Botany*, *49*(12), 2129-2137.

Havaux M., Gruszecki W.I. (1993). Heat- and light-induced chlorophyll a fluorescence changes in potato leaves containing high or low levels of the carotenoid zeaxanthin: Indications of a regulatory effect of zeaxanthin on thylakoid membrane fluidity. *Photochemistry and Photobiology*, *58*(4), 607-614.

Jia X., Zha T.S., Wu B., Zhang Y.Q., Gong J.N., Qin S.G., Chen G.P., Qian D., Kellomäki S., Peltola H. (2014). Biophysical controls on net ecosystem CO_2 exchange over a semiarid shrubland in northwest China. *Biogeosciences*, *11*(17), 4679-4693.

Jones J.B., Jr. (1991). *Kjeldahl method for nitrogen determination*. Micro-Macro publishing. Athens (Ga.).

Jönsson P., Cai Z., Melaas E., Friedl M.A., Eklundh L. (2018). A method for robust estimation of vegetation seasonality from Landsat and Sentinel-2 time series data. *Remote Sensing*, *10*(4), 635, Article 635.
Kraj W., Ślepaczuk A. (2022). Morphophysiological acclimation of developed and senescing beech leaves to different light conditions. *Forests*, *13*(8), 1333.
Lambers H., Oliveira R.S. (2019). *Plant Physiological Ecology*. Springer.
Lazarev V., Marinkovic P., Milovanovic D. (2001, 2-6 October 2001). Stress factors in forest ecosystems and their impact on condition of forests in fry. Third Balkan Scientific Conference, Sofia, Bulgaria.
Lichtenthaler H., Buschmann C., Döll M., Fietz H.-J., Bach T., Kozel U., Meier D., Rahmsdorf U. (1981). Photosynthetic activity, chloroplast ultrastructure, and leaf characteristics of high-light and low-light plants and of sun and shade leaves. *Photosynthesis Research*, *2*(2), 115–141.
Maoka T. (2020). Carotenoids as natural functional pigments. *Journal of Natural Medicines*, *74*(1), 1-16.
Naidu S.L., DeLucia E.H. (1998). Physiological and morphological acclimation of shade-grown tree saplings to late-season canopy gap formation. *Plant Ecology*, *138*(1), 27-40.
Nedkov R., Velizarova E., Avetisyan D., Georgiev N. (2020). *Assessment of forest vegetation state through remote sensing in response to fire impact*. SPIE.
Peaucelle M., Janssens I.A., Stocker B.D., Descals Ferrando A., Fu Y.H., Molowny-Horas R., Ciais P., Peñuelas J. (2019). Spatial variance of spring phenology in temperate deciduous forests is constrained by background climatic conditions. *Nature Communications*, *10*(1), 5388.
Peeters P.J. (2002). Correlations between leaf structural traits and the densities of herbivorous insect guilds. *Biological Journal of the Linnean Society*, *77*(1), 43-65.
Prieto P., Pineda M., Aguilar M. (1999). Spectrophotometric quantitation of antioxidant capacity through the formation of a phosphomolybdenum complex: specific application to the determination of vitamin E. *Analytical Biochemistry*, *269*(2), 337-341.
Ralph P.J., Smith R.A., Macinnis-Ng C.M.O., Seery C.R. (2007). Use of fluorescence-based ecotoxicological bioassays in monitoring toxicants and pollution in aquatic systems: Review. *Toxicological & Environmental Chemistry*, *89*(4), 589-607.
Retuerto R., Fernandez-Lema B., Rodriguez R., Obeso J.R. (2004). Increased photosynthetic performance in holly trees infested by scale insects. *Functional Ecology*, *18*(5), 664–669.
Roberts A.M.I., Tansey C., Smithers R.J., Phillimore A.B. (2015). Predicting a change in the order of spring phenology in temperate forests. *Global Change Biology*, *21*(7), 2603-2611.
Schieber B., Janik R., Snopkova Z. (2013). Phenology of European beech (*Fagus sylvatica* L.) along the altitudinal gradient in Slovakia (Inner Western Carpathians). *Journal of Forest Science*, *59*(4), 176-184.
Schulze E.-D., Beck E., Buchmann N., Clemens S., Müller-Hohenstein K., Scherer-Lorenzen M. (2019). *Plant Ecology*. Springer. Berlin.
Singleton V.L., Orthofer R., Lamuela-Raventós R.M. (1999). Analysis of total phenols and other oxidation substrates and antioxidants by means of folin-ciocalteu reagent *Methods in enzymology* (Vol. 299, 152-178). Academic Press.
Terashima I., Hanba Y., Tazoe Y., Vyas P., Yano S. (2006). Irradiance and phenotype: comparative eco-development of sun and shade leaves in relation to photosynthetic CO_2 diffusion. *Journal of Experimental Botany*, *57*(2), 343–354.
Urban J., Bednárová E., Plichta R., Gryc V., Vavrčík H., Hacura J., Fajstavr M., Kučera J. (2015). Links between phenology and ecophysiology in a European beech forest [Links between phenology and ecophysiology in a European beech forest] [Research Articles]. *iForest - Biogeosciences and Forestry*, *8*(4), 438-447.
Vitasse Y., Basler D. (2013). What role for photoperiod in the bud burst phenology of European beech. *European Journal of Forest Research*, *132*(1), 1-8.
Wyka T., Robakowski P., Zytkowiak R. (2007). Acclimation of leaves to contrasting irradiance in juvenile trees differing in shade tolerance. *Tree Physiology*, *27*(9), 1293-1306.
Zha T.-S., Wu Y.J., Jia X., Zhang M.Y., Bai Y.J., Liu P., Ma J.Y., Bourque C.P.-A., Peltola H. (2017). Diurnal response of effective quantum yield of PSII photochemistry to irradiance as an indicator of photosynthetic acclimation to stressed environments revealed in a xerophytic species. *Ecological Indicators*, *74*, 191-197.